BRNO UNIVERSITY OF TECHNOLOGY

FACULTY OF CIVIL ENGINEERING

PROPERTIES OF STEEL APPLIED IN CIVIL ENGINEERING INDUSTRY IN SELECTED COUNTRIES: S235 AND S355

BACHELOR THESIS

AUTHOR Ignacio Rodríguez Sánchez

SUPERVISOR Assoc. Prof. Stanislav Seitl
SUPERVISOR SPECIALIST: Ing. Petr Miarka

BRNO 2019

ABSTRACT

This thesis is focused in the comparison of the steels S235 and S355 grades properties from various countries of the Europe Union. This has been done comparing their chemical composition, mechanical properties, strength properties and selected fatigue properties such as *S-N* curves (Wöhler curves) and Crack Propagation Rate curves.

These two grades of steels were compared in order to study the influence of the material in their fatigue properties. The data used for the bachelor's thesis was obtained from articles focused of selected steel grades and from experimental program performed on Institute of Physics of Materials ASCR in cooperation with Faculty of Civil Engineering, Brno University of Technology.

KEYWORDS

Steel, S235, S355, mechanical properties, chemical composition, strength of material, fatigue properties, *S-N* curve, crack propagation rate.

RESUMEN

Esta tesis está enfocada en la comparación de las propiedades de los aceros S235 y S355 en varios países de Europa. De esta manera, se ha realizado una comparación entre su composición química, propiedades mecánicas y sus propiedades a fatiga como son las curvas *S-N* (curvas de Wöhler) y las velocidades de propagación de grietas.

Estos dos tipos de aceros han sido comparados con el objetivo de estudiar la influencia del material en las propiedades a fatiga de éstos.

La información usada en este proyecto fue obtenida en base a publicaciones de diferentes artículos sobre estos tipos de aceros y de un programa experimental realizado en el Institute of Physics of Materials ASCR en cooperación con la Facultad de Ingeniería Civil de Brno University of Technology.

PALABRAS CLAVES

Acero, S235, S355, propiedades mecánicas, composición química, resistencia del material, propiedades a fatiga, curvas *S-N*, velocidades de propagación de grietas.

BIBLIOGRAPHIC CITATION

Ignacio Rodríguez Sánchez Properties of steel applied in civil engineering industry in selected countries: S235 and S355. Brno, 2019. 46 p., 0 p. of attachments. Bachelor Thesis. Brno University of Technology, Faculty of civil engineering and University of Oviedo, Supervisor: *Assoc. Prof. Stanislav Seitl*. Supervisor Specialist: Ing. Petr Miarka.

ACKNOWLEDGEMENT

The thesis was prepared under support of ERASMUS Plus programme and in framework of the Czech Science Foundation under the contract No. 17-01589S. This paper has been worked out under the “National Sustainability Programme I” project “AdMaS UP – Advanced Materials, Structures and Technologies” (No. LO1408) supported by the Ministry of Education, Youth and Sports of the Czech Republic.

I would like to thank the invaluable help of my tutors Stanislav Seitl, Petr Miarka and María Jesús Lamela, who made it possible to carry out this project. Also, to my family, it would not have been able to carry out this project without their help and support.

INDEX

1. INTRODUCTION

The importance of the material has been crucial in the civil engineering industry of the past centuries, and nowadays keeps being one of the main factors that makes the difference in this sector.

Buildings and structures including bridges, dams, roads and canals have been built since pre-history.

At the beginning of the human history, buildings were made in a precarious way using leaves or branches. Over time, materials like timber, clay or stone were started to use. After this came the age of concretes and bricks. Finally, with the industrial revolution, material such as metal and steel were introduced into this.

Today, we see buildings made of bricks, concrete, wood, steel and glass. These materials are no more a revolution.

Here is an example of how the Civil Engineering has changed over time.

Figure 2. Roman bridge built with stone with an arch as its basic structure. (see e.g. Cangas de Onís, Asturias, Spain) retaken from [1]

Figure 3. Horreo raised from the ground by pillars ending in flat staddle stones to prevent access by rodents. (Asturias, Spain), retaken from [2]

Figure 1. Congress Palace of Oviedo made of reinforcement concrete (Oviedo, Asturias, Spain), retaken from [3]

The demand for steel as a building material is growing within the construction industry. Steel's high strength, ductility, adaptation to prefabrication, speed of erection, etc., have always been attractive characteristics to consultants and developers. In today's "fast tracked" construction projects, where time and schedule are of essence, these qualities become decisive in choosing the type of structure to be built.

One of the main steel properties are the yield strength (σ_y), the ultimate strength (σ_u), the modulus of Elasticity (*E*), the elongation (*A*%) and the chemical composition.

Even though steel has very good properties, it has its defects. Here is where fatigue appears.

In general, fatigue is perhaps the most important failure mode to be considered in mechanical and structural design. For some products, fatigue accounts for more than 80% of all observed service failures.

Moreover, fatigue and fracture failures are sometimes catastrophic, occurring without warning and causing significant property damage and loss of life. Design for fatigue avoidance is difficult, because the fatigue stresses are complicated random processes, the fatigue process is influenced by many factors, and many of the factors are subject to considerable uncertainty.[4]

The study of the fatigue properties of materials was begun by Wilhelm Albert, which, in 1837, thorough the use of experimental work, publishes the first article about fatigue in history, demonstrating that fatigue was not associated with an accidental overload, but was dependent on load and number of cycles. [5]

After him, several investigators developed different methods in predicting the fatigue life of materials, such as August Wöhler, which in the middle of the 19th century, marks the first systematic investigation of *S-N Curves*, also known as Wöhler curves to characterise the fatigue behaviour of materials. [6]

On the other hand, in 1910, O. H. Basquin proposes a log-log relationship for *S-N* curves, using Wöhler's test data, [7] and, in the middle of the 20th century, Waloddi Weibull proposes an *S-N* model curve, and his most famous research, the Weibull distribution. [8] Finally, several famous researchers, such as A. M. Miner, L. F. Coffin and S. S. Manson, with the fatigue crack-growth explanation, P. C. Paris with the method for predicting the rate of growth of individual fatigue cracks or A. F. Canteli have found various methods of fatigue life prediction.

2. THEORETICAL BACKGROUND

Theoretical information of steels will be based first on its mechanical characteristics and European characterization, in order to understand how to distinguish them and why are defined. After this, the tensile test will be explained, since basic information of steel are obtained from this experiment.

Finally, fatigue properties and fracture mechanics model will be explained with the aim of understanding the influence of fatigue in steels through *S-N* curves and crack propagation rate curve.

2.1. Steel grades

Structural steel is a standard construction material, made from specific grades of steel and formed in a range of industry standard cross-sectional shapes (or 'Sections'). Structural steel grades are designed with specific chemical compositions and mechanical properties formulated for particular applications.

Depending on the manufacturing process, chemical composition and relevant application, further letters and classifications might be used to reference grades/products of structural steel.

There are many standards that provides information about the properties of the steels, such as the Japanese Industrial Standards (JIS), German (DIN) standard, China (GB) standard or the International Organization for Standardization (ISO). In our case we will realize the comparison with the European Standard (EN 10025).

European Standard steel grades fall into two categories:

1. Steel specified by purpose of use and mechanical properties.
2. Steel specified by chemical composition. [9]

Basic grade designations for category 1 steels (-see Table 1-) consist of a single letter (designating application) then a number signifying the mechanical property dictated in the standard for that application designation.[9]

Application symbol	Meaning	Mechanical property
S	Structural steel	Minimum yield strength
P	Steel for pressure lines and vessels	Minimum yield strength
L	Steel for pipe and tube	Minimum yield strength
E	Engineering steels	Minimum yield strength
B	Steel for reinforced concrete	Characteristic yield case
R	Steel for rail use	Minimum yield case
H	High Tensile Strength Flat products	Minimum yield case
D	Flat Products for Cold Forming	
T	Tin mill Products	Nominal yield case
M	Electrical Steel	

Table 1. Basic grade designations for category 1 steels, data obtained from [10]

In addition to the above category codes there are symbols that can be added to the grade code to identify any additional compositional requirements, delivery conditions, mechanical properties and so on.

These values depend solely on the type/application code given in the first part of the code and are so numerous as to be impossible to indicate here.

Impact Resistance		Temperature	
Impact code	Testing strength	Temperature code	Testing temperature
J	27 J	R	Room temperature
K	40 J	O	0 °C
L	60 J	2	-20 °C
		3	-30 °C
		4	-40 °C
		5	-50 °C
		6	-60 °C

Table 2. Impact resistance and temperature codes for category 1 steels, data obtained from [9]

Code	Condition
A	Annealed
QT	Quenched and tempered
N	Normalised
SR	Stress relieved
C	Cold worked
U	Untreated

Table 3. Delivery condition codes for category 1 steels, data obtained from [9]

2.2. Mechanical properties

Over the years, the importance of the steel has been increasing due to many factors. Steel's great resistance to heat transfer, good fatigue properties, durability, tenaciousness and also appearance makes it one of the bests options in civil engineering industry.

2.2.1 Tensile test

The tensile test is the most important and known mechanical test, since is the only one that allows to obtain the material's behaviour curve and its fundamental mechanical properties.

A specimen is placed between two grips which clamps the material, moved vertically by a load cell with a constant speed. One of the ends of the specimen is fixed and the other one is gripped. The loads are applied through the threaded or shouldered ends.

The important parameters of the specimens are the gage length (L_0) and the initial cross-section area (S_0). The gage length is the region over which measurements are made and is centered within the reduced section. The distances between the ends of the gage section and the shoulders should be great enough so that the larger ends do not constrain deformation within the gage section, and the gage length should be great relative to its diameter. [11]

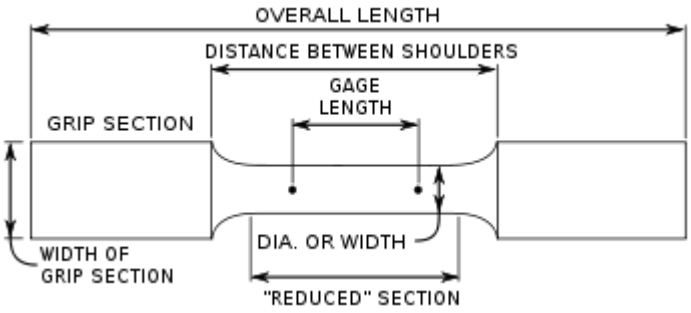

Figure 4.Specimen used in Tensile test, retaken from [12]

After a certain amount of the plastic deformation of the material, due to the reorientation of the crystal structure, an increase in load is observed with increase of strain. This range is called the strain hardening range. After a little increase in load, the specimen eventually fractures.

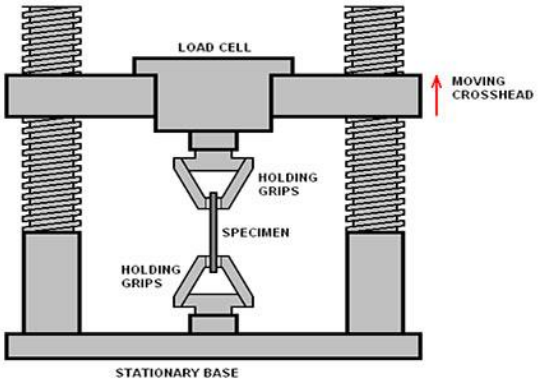

Figure 5.Tensile test machine, retaken from [13]

The results of the tensile tests are used in selecting materials for engineering applications, such as the stress-strain diagrams, yield strength (σ_y), ultimate strength (σ_u), poison's ratio (υ), modulus of Elasticity (E) or the elongation ($A\%$).

Furthermore, it also has a great importance, due to the capacity of predicting how a material will perform its use or to determine if it verifies the requirements or specifications given from the standards. [14]

2.2.2 Stress-strain curves

With the increasing use of advanced computational and analytical methods in structural engineering, there is a crucial need for accurate representations of the key input parameters.

Representation of the full stress-strain curve is particularly important in analytical, numerical or design models for scenarios in which large plastic strains are encountered. This stress-strain curve is obtained by the tensile test. [15]

2.2.2.1 “Engineering” stress-strain curves

The engineering tensile test is widely used to provide basic design information on the strength of materials and as an acceptance test for the specifications of materials.

The engineering measures of stress and strain, denoted in this module as σ_e and ε_e respectively, are determined from measuring the load and deflection using the original specimen cross-section area S_0 and length L_0 as:

$$\sigma_e = \frac{F}{S_0} \tag{1}$$

$$\varepsilon_e = \frac{\Delta L}{L_0} \tag{2}$$

When the stress σ_e is plotted against the strain ε_e, an engineering stress-strain curve such as shown in Graph 1 is obtained.

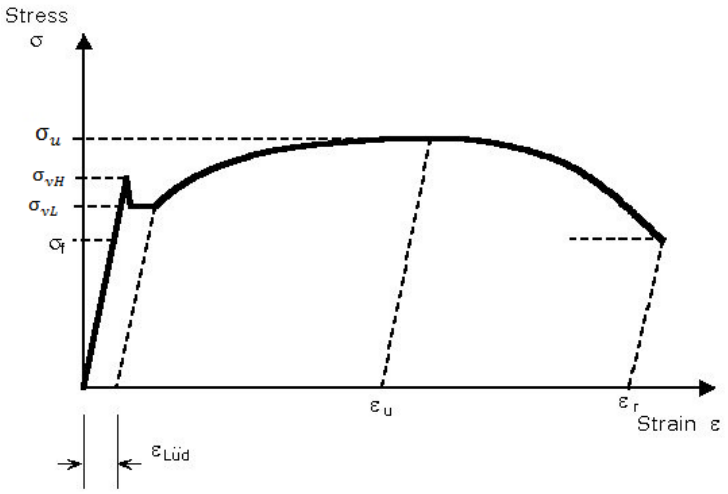

Graph 1. Engineering stress-strain curves for mild steel, retaken from [17].

In the early (low strain) portion of the curve, many materials obey Hooke’s law to a reasonable approximation, so that stress is proportional to strain with the constant of proportionality being the modulus of Elasticity or Young’s modulus (*E*):

$$\sigma_e = E \cdot \varepsilon_e, \tag{3}$$

$$E = tg(\alpha). \tag{4}$$

As strain is increased, many materials eventually deviate from this linear proportionality, the point of departure being termed the proportional limit. This nonlinearity is usually associated with stress-induced “plastic” flow in the specimen. Here the material is undergoing a rearrangement of its internal molecular or microscopic structure, in which atoms are moved to new equilibrium positions.

At this point, if the load is removed while the material is at the plastic term, there will be a permanent plastic deformation.

2.2.2.2 True stress-strain curves

True stress-strain curves are used for accurate definition of plastic behaviour of ductile materials by considering the actual (instantaneous) dimensions.

During yield and the plastic-flow regime following yield, the material flows with negligible change in volume; increases in length are offset by decreases in cross-sectional area.

$$\sigma' = \frac{F}{S} = \frac{F}{S_0}(1 + \varepsilon) \tag{5}$$

$$\varepsilon' = \frac{\Delta L}{L} = Ln(1 + \varepsilon) \tag{6}$$

These equations can be used to derive the true stress-strain curve from the engineering curve, up to the strain at which necking begins. [16]

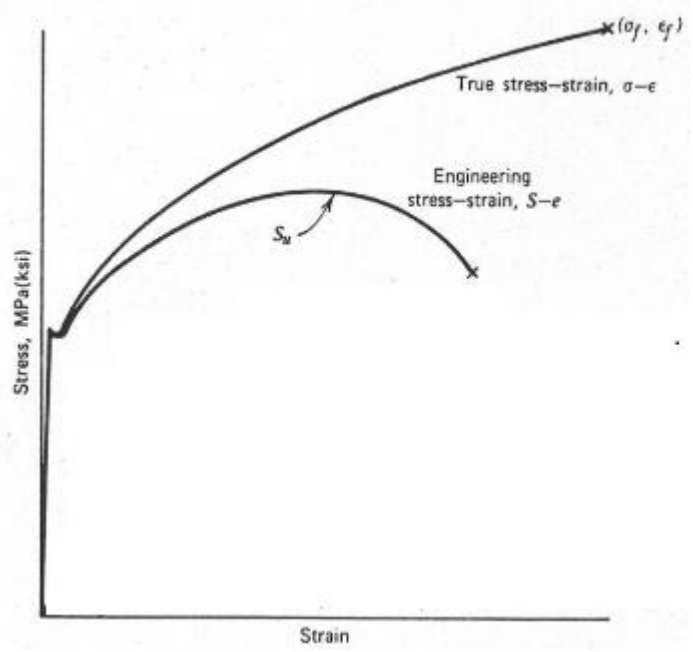

Graph 2. Comparison of true and engineering stress-strain curves for mild steels, retaken from [18]

There is an approximate linear relationship between true stress and true strain when plotted on log-log scale, the Hollomon's equation:

$$\sigma' = K\varepsilon'^{n} \tag{7}$$

where σ' is the true stress, ε' is the true strain, n is the strain-hardening exponent and K is the strength coefficient. In the Hollomon's expression, the strain-hardening exponent measures the ability of a metal to strain-harden, larger magnitudes indicate larger degrees of strain hardening. The strain-hardening exponent and the strength coefficient are both determined from the logarithm of the true strain in the region of uniform elongation.

Total elongation in a material during deformation has been known to originate from elastic and plastic contributions. Therefore, the elastic and plastic strain can be evaluated from the expressions given below:

$$\varepsilon' = \varepsilon_{el} + \varepsilon_{pl} \tag{8}$$

$$\varepsilon_{el} = \frac{\sigma'}{E} \tag{9}$$

$$\varepsilon_{pl} = \alpha\left(\frac{\sigma'}{\sigma_y}\right)^{\frac{1}{n}} \tag{10}$$

$$\varepsilon' = \frac{\sigma'}{E} + \alpha\left(\frac{\sigma'}{\sigma_y}\right)^{\frac{1}{n}} \tag{11}$$

where α is also a characteristic property of the material.

This type of true stress-strain relationship is often referred to as the Ramber-Osgood relationship. [19]

2.3. Fatigue

Fatigue is the progressive, localized, and permanent structural change that occurs in a material subjected to repeated or fluctuating strains at nominal stresses that have maximum values less than (and often much less than) the tensile strength of the material. Fatigue may culminate into cracks and cause fracture after enough fluctuations.

Fatigue damage is caused by the simultaneous action of cyclic stress, tensile stress, and plastic strain. If any of these three is not present, a fatigue crack will not initiate and propagate. The plastic strain resulting from cyclic stress promotes crack growth (propagation). Careful measurement of strain shows that microscopic plastic strains can be present at low levels of stress where the strain might otherwise appear to be totally elastic.

Although compressive stresses will not cause fatigue, compressive loads may result in local tensile stresses. [20]

Thorough the study of fatigue, several parameters have been used to define the different types of fatigue cycles. Most commonly used are σ_{max} and σ_{min}, but nevertheless, other parameters are highly used as well:

Mean stress (σ_m): The mean stress is the algebraic average of the maximum stress and the minimum in one cycle.

$$\sigma_m = \frac{(\sigma_{max}+\sigma_{min})}{2} \tag{12}$$

Stress range (Δσ): Is the algebraic difference between the maximum stress and the minimum stress in one cycle.

$$\Delta\sigma = \sigma_{max} - \sigma_{min} \tag{13}$$

Stress amplitude (σ_a): Is one-half the range of the stress.

$$\sigma_a = \frac{\sigma_{max}-\sigma_{min}}{2} \tag{14}$$

Stress ratio (R): Is the algebraic ratio of two specified stress values in a stress cycle.

$$R = \frac{\sigma_{min}}{\sigma_{max}} \tag{15}$$

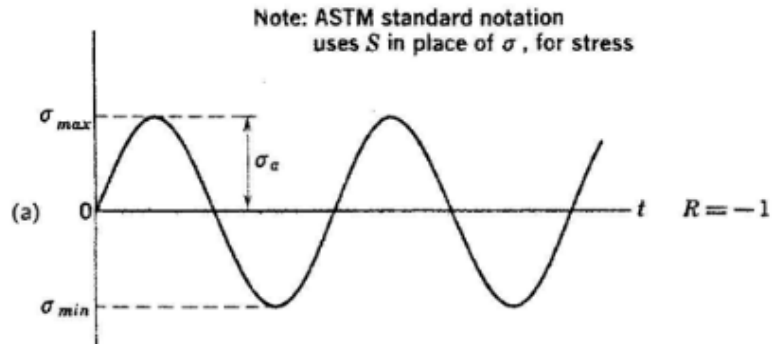

Graph 3. Fully reversed stress cycle, in which σ_m=0, retaken from [21]

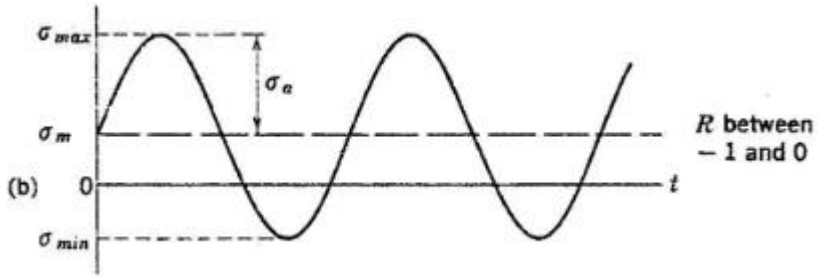

Graph 4. Repeated stress cycle, in which σ_m=σ_a, retaken from [21]

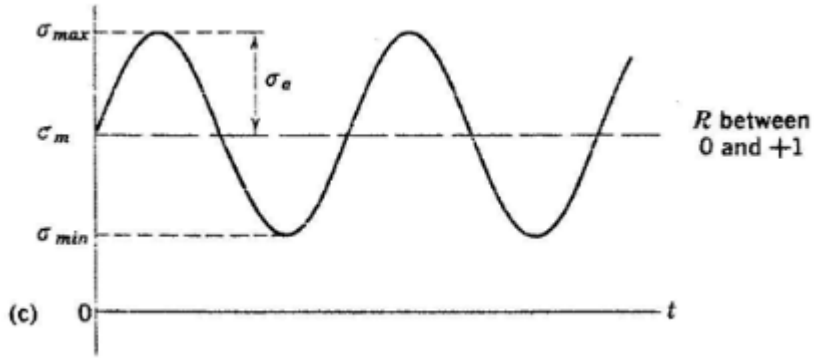

Graph 5. Fluctuating stress cycle, in which σ_{min} and σ_{max} are >0, retaken from [21]

2.3.1 Fatigue regimes

Several regimes are classified depending on the number of cycles an element is subjected to in fatigue procedures:

- Very Low-Cycle Fatigue (VLCF): $N_f < 10^2$ cycles
- Low-Cycle Fatigue (LCF): $10^2 < N_f < 10^3$ cycles
- High-Cycle Fatigue (HCF): $10^3 < N_f < 10^7$ cycles
- Very High-Cycle Fatigue (VHCF): $N_f > 10^7$ cycles

Usually, mechanical engineering structures are designed for high- (HCF) and low-cycle fatigue (LCF) regimes. However, civil engineering structures such as bridges, are designed for high-cycle fatigue (HCF) regimes.

2.3.2 Traditionally used models for evaluation of fatigue properties

Characterization of the fatigue behaviour of structures by *S-N* techniques is performed by testing, preferably under constant amplitude cycles, of several test coupons at different maximum fatigue loads. [22] Alternatively, the fracture mechanics-based approach, allows the crack propagation from an initial crack size a_0, to a final crack size a_f to be predicted using fatigue crack growth curves. [23]

2.3.2.1 *S-N* curves

The relationship between stress range ($\Delta\sigma$) or stress amplitude (σ_a) and cycles to failure (N_f) in a logarithmic scale has been used for a long time to characterize the fatigue behaviour of metals and fatigue design. The influence of a wide range of variables on fatigue behaviour has been studied, including mean stress and frequency.

S-N curves often exhibit significant scatter. This scatter has required that a statistical approach to fatigue reliability be taken and this has important implications for our understanding of the structural integrity of metal components. [24]

Not every steel behaves in the same way. Many factors influence in fatigue failures when it occurs. Fatigue limit or (endurance limit) is the value of the stress below which a material can presumably endure an infinite number of stress cycles, that is, the stress at which the *S-N* diagram becomes and appears to remain horizontal. [20]

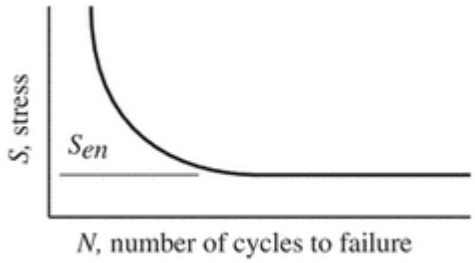

Graph 6. S-N curve with endurance limit, retaken from [25].

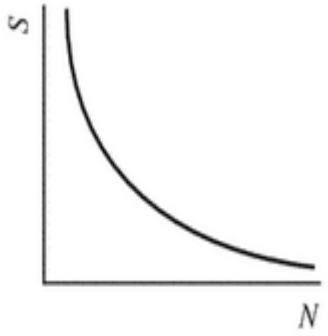

Graph 7. S-N curve, retaken from [25].

S-N curves were originally proposed by Basquin and adopted in the design codes, given by following expression:

$$\sigma = A \cdot N^B \tag{16}$$

where the parameters *A* and *B* denote the independent term and slope, respectively, of the resulting straight line in double logarithmic scale. The scatter of the test result at the same level of loading is a characteristic inherent to the fatigue phenomenon due to several factors, such as material defects during the process of extrusion and machining process of specimens. [23]

2.3.2.2 Fracture mechanics-base model

Until recent years, little effort had been devoted to the experimental determination of the laws governing the rate of growth of a fatigue crack; in fact, no accurate quantitative experimental data had been published before 1953. [26]

2.3.2.2.1 Compact tension specimen

Regarding the American Society of Testing and Materials (ASTM), the compact tension specimen (*CT*), is a notched sample used to create a fatigue crack by cycled loads.

In *CT* specimen, due to tensile loads, the crack will open symmetrically in mode I, which will be explained after. Figure 6 shows the *CT* specimen.

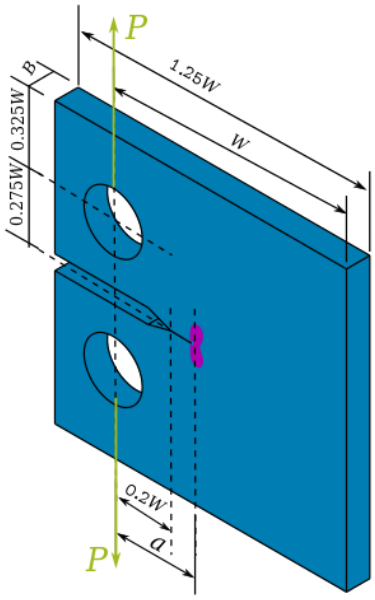

Figure 6. *CT* specimen, retaken from [27]

2.3.2.2.2 Modes of crack growth

Prior to start with crack propagation rate curve, it is necessary to explain that there are three basic modes of crack surface displacements which can cause crack growth; these are shown in Figure 7:

I. The opening mode: The crack surface move directly apart.

II. The edge sliding mode: The crack surface moves normal to the crack front and remain in the crack plane.

III. The shear mode: The crack surface moves parallel to the crack front and remain in the crack plane.

The superimposition of these three models are enough to describe the most general cases of crack surface displacement. [26] In this bachelor thesis, only mode I is considered.

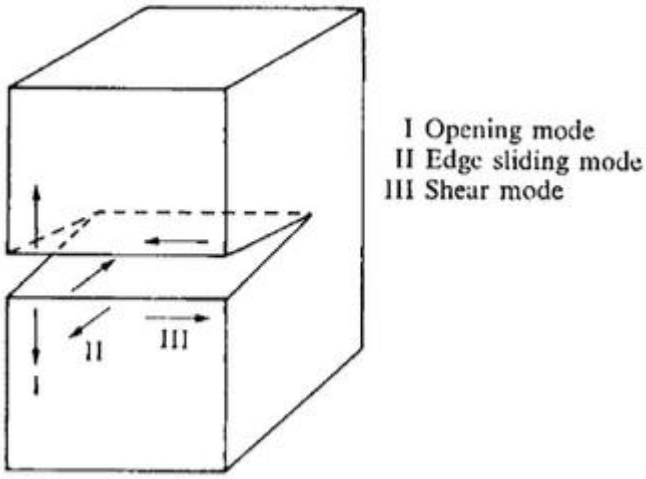

Figure 7. Modes of crack growth, retaken from [26]

2.3.2.2.3 Crack propagation rate curve

Paris and Erdogan (1963) suggested that the most relevant parameter to describe the fatigue crack growth was the range of the stress intensity factor ΔK, which is schematically described in graph 8 as a log-log scale. Three distinct regions are indicated: 1) the well-known threshold region, 2) intermediate region, and 3) the failure region. [28]

Where

$$\Delta K = (K_{max} - K_{min}) = \Delta\sigma \cdot Y \sqrt{\pi \cdot a} \tag{17}$$

In which Y represents the function depending on the geometrics and loading conditions, and a is the crack length.

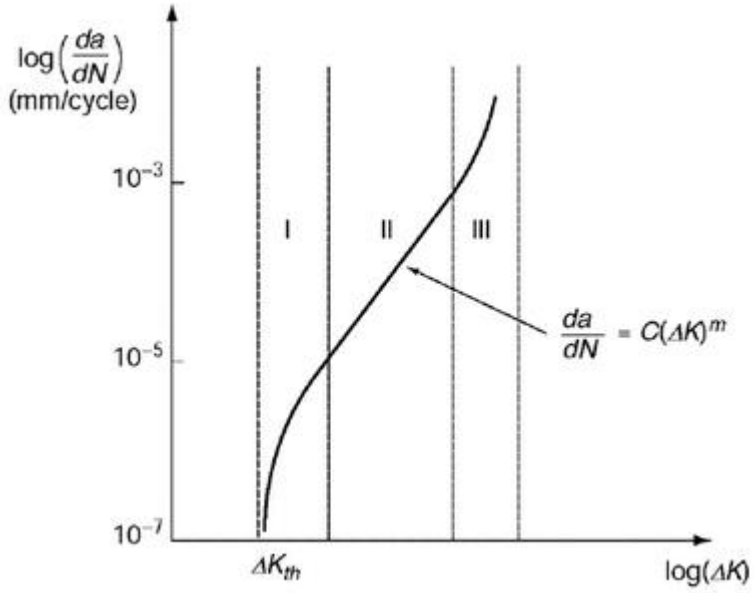

Graph 8. Crack growth rate curve, retaken from [29]

Region I correspond with low values of ΔK applied, in which fatigue crack growth rate, da/dN, is equally small. In this region, the most important parameter is the threshold of the stress intensity factor range below which no fatigue crack growth should occur ΔK_{th}.

In region II, the crack growth rate da/dN can be approximately linear related to the stress intensity factor range ΔK in the log-log scale plot. The Paris law for crack growth is

$$\frac{da}{dN} = C \cdot \Delta K^m \tag{18}$$

Where C and m are material constants. [29]

Finally, in region III when ΔK is large, the crack growth accelerates and in short time the complete break of the material will take place.

The importance of the Paris law is undeniable, since it can predict crack growth in every material.

Generally, to simplify calculations, regions I and III are usually despised. So, it is possible to estimate the fatigue life of the material utilizing only Paris law in region II.

Integrating the equation (18) gives:

$$\int_{Ni}^{Nf} dN = N_f - N_i = \int_{a_0}^{ac} \frac{da}{C \cdot \Delta K^m} \tag{19}$$

where a_0 represents the initial crack length, a_c the final crack length, N_i the number of cycles at the initial crack length and N_f the number of cycles at the final crack length.

3. AIMS

The aim of this thesis is to collect information about properties of steels S235 and S355 in various countries of the Europe Union and compare them in order to understand their fatigue properties.

To this end, static properties, such as chemical composition, mechanical properties and strength properties are measured from steels S235 and S355 with smooth specimens to compare among them and with the standards given by the European standard EN10025-2:2004.

Moreover, *S-N* curves and crack propagation rate from S235 and S355 of selected countries have been evaluated through Wöhler's curves and crack propagation rate curves in order to compare the influence of the material in their fatigue properties.

4. Selected Materials used in civil engineering area

The construction/structural steels that are widely explained (see chapter1-INTRODUCTION-) lay among low strength and mild strength steels. This bachelor thesis aims to compare the fatigue properties of selected steel grades. At the same time, mechanical properties and chemical composition are key part in the way that the steel behaves (see chapter 3 -AIMS-).

In the following part of Bachelor thesis, the focus was done in steels S235 and S355 grades.

4.1. Steel S235 grade

The S235 steel sheet is a structural steel that complies with the European standard of EN 10025-2:2004. S235 structural steel sheet is made of common carbon steel that can be used in a very wide range of manufacturing processes, such as mechanical engineering industry and buildings.

This sheet has an excellent formability, but its use is limited in applications that require structural specifications of greater weight bearing.

S235 is named based on its minimum yield strength of 235 MPa, however, the yield strength reduces when the thickness is increased above 16 mm for flat products and hollow sections.

Steel S235 has several names depending on which country is used.

Table 4 shows an example of steel S235J2G3 designation in various countries:

Steel S235J2G3 [30]							
EN 10025-2	Spain	Poland	Italy	Germany	Portugal	U. K.	China
1.0116	AE 235 D	St3w	Fe 360 D	St 37-3N	Fe 360 D	40D	Q 235D

Table 4. Steel S235J2G3 equivalent designations, data obtained from [30].

4.1.1 Static properties

Mechanical properties of structural steel are fundamental to its classification and hence application.

The yield strength (σ_y) of structural steel is the stress the material can withstand without permanent deformation. This is not a sharply defined point. Yield strength is the stress which cause a permanent deformation of 0.2% of the original dimension.

Moreover, ultimate strength (σ_u) of Structural steel relates to the point of maximum stress that the material can withstand.

From this material, we will compare the steel S235J2G3 from Poland, Italy and Germany with the European standard EN 10025-2:2004. Monotonic properties of this structural steels are compared in Table 6:

	EN 10025-2:2004 [31]	Poland [32]	Italy [33]	Germany [34]
Min σ_y [MPa]	235	307	282	277
σ_u [MPa]	360/510	461	412	415
E [GPa]	-	207	-	-
A [%]	-	33.8	37	43

Table 5. Monotonic properties comparison of steel S235J2G3 in various countries.

4.1.2 Chemical composition

Chemical composition of structural steel is extremely important and highly regulated. It is a fundamental factor which defines the mechanical properties of the steel material.

Table 6 shows the maximum values of chemical composition of steel S235J2G3 given by EN 10025-2:2004.

	C [max %]	Mn [max %]	Si [max %]	P [max %]	S [max %]	N [max %]	Cu [max %]	CEV [max %]
EN 10025-2:2004 [31]	0.17	1.5	-	0.025	0.025	-	0.55	0.40

Table 6. Chemical composition of steel S235J2G3, data obtained from [31].

In order to compare their chemical composition, it is very important that the values of the chemical elements do not exceed the maximum value given by the standards.

In Table 7, chemical composition of steel S235J2G3 from Poland, Italy and Germany are compared among them and with the European Standard EN 10025-2:2004.

Carbon, manganese, silicon, phosphorus, sulphur and aluminium composition appear to be in all S235 steels, and even with different values seems to be important parameters to grant good mechanical properties.

These values give us information that the same steel, in every country has its own characteristics due to the soil composition, which grants different properties to its use in the civil engineering industry.

	EN 10025-2:2004 [31]	Poland [32]	Italy [33]	Germany [34]
C [max %]	0.17	0.16	0.164	0.084
Mn [max %]	1.5	0.81	0.397	0.658
Si [max %]	-	0.22	0.018	0.169
P [max %]	0.025	0.01	0.012	0.02
S [max %]	0.025	0.02	0.008	0.009
N [max %]	-	-	0.0033	-
Cu [max %]	0.55	-	-	-
Al [max %]	-	0.04	0.035	0.039
Cr [max %]	-	0.13	-	0.03
Ni [max %]	-	0.09	-	0.035
Mo [max %]	-	-	-	-
Cev [max %]	0.4	-	-	-

Table 7. Chemical composition comparison of steel S235J2G3 in various countries.

4.1.3 Fatigue properties

Knowledge of fatigue resistance of the material plays a key role during design and maintenance of the civil engineering structures.

Steel S235 fatigue properties of various specimens are included in the following chapter. It is important to remark that steel S235 is less commonly used than other structural steels.

4.1.3.1 *S-N* curves

The *S-N* curves approach is an established fatigue prediction technique used in many fields of applications. Common *S-N* curves are performed with $\Delta\sigma$-*N* or σ_a-*N* experimental data.

In steel S235 case, *S-N* curves found in articles of the literature were plotted in σ_a-*N*, being σ_a the stress range and *N* the number of cycles in a logarithmic scale.

It should be noted that there was not many valid information for steel S235, due to its less use in the civil engineering industry compared to the steel S355, even being a mild steel as well. There were only two S235 steels that met the requirements.

First steel used is a S235JR from Poland. Figure 8 shows the geometry of the smooth specimen used in tests. Specimen has a cross-section area S_0 of 176.71 mm^2.

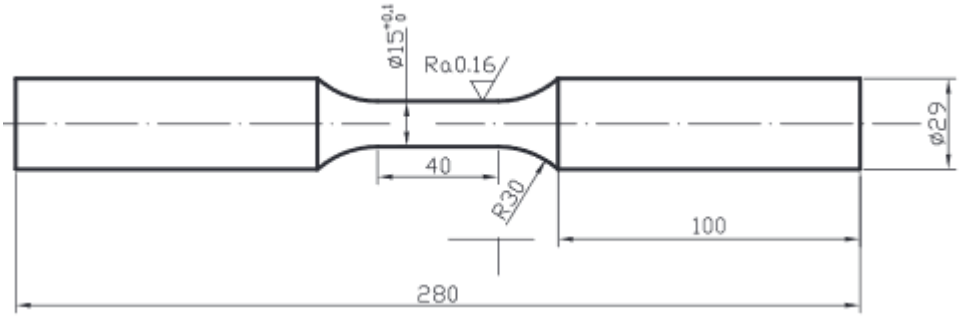

Figure 8. Geometry of smooth cylindrical specimen made of S235JR from Poland, retaken from [35]

The fatigue test of the smooth specimen was performed using cyclic loading with zero mean stress (*R*=-1). Also, specimens were tested with a force up to 400 kN and a frequency of 5Hz.

S-N curve from experimental data was plotted in order to understand its fatigue behaviour and compare it to other specimens, in which measurements of fatigue life in steel component were made based on the principles of Basquin's law.

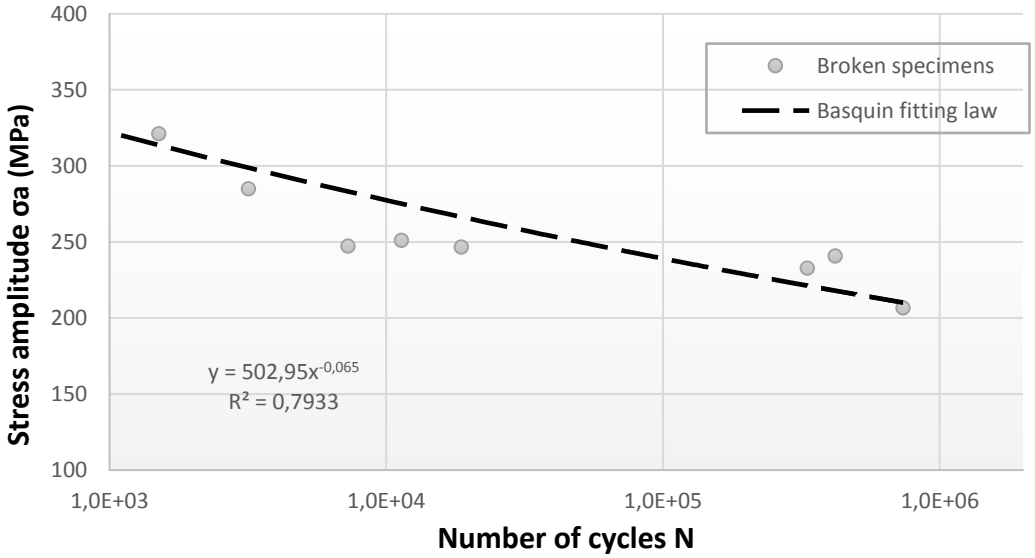

Graph 9. *S-N* curve of steel S235JR from Poland, data adopted from [35]

Table 8 shows the results of fatigue experiment at high number of cycles.

Poland [35]				
N [cycles]	1.0E+04	1.0E+05	1.0E+06	1.0E+07
σ_a [MPa]	276.391	237.97	-	-
σ_a/σ_u σ_u=423 [MPa]	0.653	0.562	-	-

Table 8. Stress evaluation at High-Cycle Fatigue regime of S235JR from Poland.

Relationship between stress amplitude σ_a and ultimate strength σ_u shows an apparently normal behaviour of the specimen until failure, since the relationship is <1.

S-N curve provides us information between the stress amplitude and the cycles to failure, in which broken specimens at high number of cycles show an apparently normal value of stress amplitude. Also, the specimens show a descendant slope with little inclination at high number of cycles as well.

Second and last S235 steel used in this bachelor thesis is a S235 from Portugal. Figure 9 shows the smooth specimen's geometry used in tests and Table 9 specifies the dimensions adopted for the steel S235. The specimen has a cross-section area S_0 of 30 mm^2.

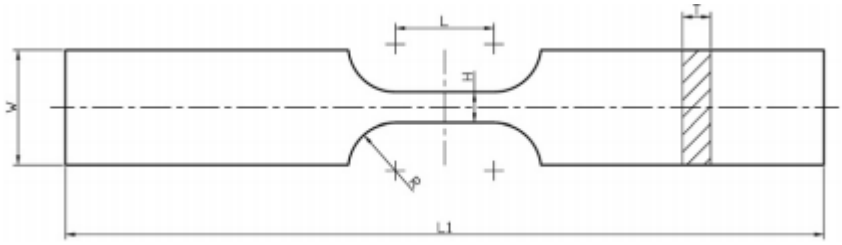

Figure 9. Geometry of smooth plane specimen made of S235 from Portugal, retaken from [36]

Specimen	W [mm]	T [mm]	L [mm]	L1 [mm]	H [mm]	R [mm]
S235	20	5	15	135	6	12

Table 9. Nominal dimension of smooth specimen made of S235 from Portugal. [36]

The fatigue tests of the specimen were performed using cyclic loading with stress ratio *R*=0. Specimens were tested with a force up to 100 kN and a frequency that adjusted to results.

S-N curve from experimental data was plotted in order to analyse its fatigue behaviour and to compare it with other specimens. Basquin's law principles were used to measure the experimental data.

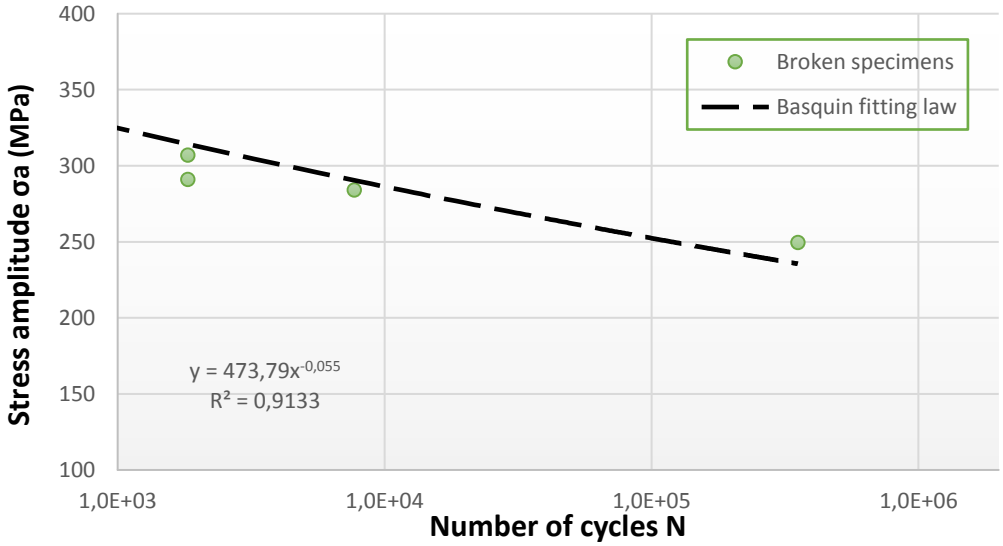

Graph 10. S-N curve of steel S235 from Portugal, data obtained from [36]

Table 10 shows the results of the experimental data at high number of cycles.

Portugal [36]				
N **[cycles]**	**1.0E+04**	**1.0E+05**	**1.0E+06**	**1.0E+07**
$\boldsymbol{\sigma_a}$ **[MPa]**	324.030	285.486	-	-
$\boldsymbol{\sigma_a/\sigma_u}$ $\boldsymbol{\sigma_u}$=435 [MPa]	0.578	0.509	-	-

Table 10. Stress evaluation at High-Cycle Fatigue regime of S235 from Portugal.

Since there is no information available of the ultimate strength σ_u in the literature, mean value of σ_u given by the standards was used (σ_u= 435 MPa) in order to at least approximate the evaluation between the stress amplitude σ_a and the ultimate strength σ_u. Reasonable values of this relationship were obtained as well. At the same time, *S-N* curve provides us information in which appears to be a progressive descendant line, with common stress amplitude's values for broken specimens at high number of cycles for S235 steel.

4.1.3.2 *S-N* curve comparison for selected specimens.

S-N comparison between S235JR from Poland and S235 from Portugal has not been possible due to several factors.

To begin with, an essential factor to compare various specimens is the stress ratio *R*. It is important that the specimens must be loaded with the same type of cycle; if not, fatigue crack may propagate in another way, as tension and compression stresses are completely different.

Finally, geometry of the specimens is not the same; first one is cylindrical and the second one is plane. This supposes an alteration of the stresses suffered of each specimen due to the stress concentrators that plane specimens have in comparison with rounded ones.

4.2. Steel marked S355

S355 steel sheet is a structural steel of high strength and mild alloy that complies with the European standard of EN 10025-2:2004.

S355 is used in almost every facet of structural fabrication. Typical applications include:

- Structural steel works, such as bridge components or components for offshore structures.
- Power plants.
- Mining and earth-moving equipment.
- Load-handling equipment.
- Wind tower components.

S355 is named based on its minimum yield strength of 355 MPa, however, the yield strength reduces when the thickness is increased above 16 mm for flat products and hollow sections.

Steel S355 grade has several names depending on which country are used/produced.

Here is an example of steel S355J2G3 designation in various countries from world:

Steel S355J2G3 [30]							
EN 10025-2	Spain	Poland	Italy	Germany	Portugal	U. K.	China
1.0570	AE 355 D	10HNAP	Fe 510 D	St 52-3N	Fe 510 D	50D	-

Table 11. Steel S355J2G3 equivalent designations, data obtained from [30].

4.2.1 Static properties

As it was explained before, mechanical properties of steels are fundamental to its classification and hence applications.

The most important parameters to take in count are the yield strength (σ_y) and the ultimate strength (σ_u), which have been compared from countries such as Spain, Poland, Germany and Portugal with the European standard EN 10025-2:2004.

	EN 10025-2:2004 [31]	Spain [37]	Poland [38]	Italy [39]	Germany [34]	Portugal [40]
Min σ_y [MPa]	355	386	418	455	362	419
σ_u [MPa]	470/630	689	566	620	566	732
E [GPa]	-	206	215	-	206	-

Table 12. Monotonic properties comparison of steel S355J2G3 in various countries.

4.2.2 Chemical composition

Chemical composition of structural steels is extremely important and highly regulated. It is a fundamental factor that defines the mechanical properties of the steel material.

In Table 13 is shown the maximum values of chemical composition of steel S355J2G3 given by EN 10025-2:2004.

	C [max %]	Mn [max %]	Si [max %]	P [max %]	S [max %]	N [max %]	Cu [max %]	CEV [max %]
(S355J2G3) EN 10025-2:2004 [31]	0.2	1.6	0.55	0.03	0.03	0.012	0.55	0.47

Table 13. Chemical composition of steel S355J2G3, data obtained from [31].

In order to compare their chemical composition, it is very important that the values of the chemical elements do not exceed the maximum values given by the standards.

Table 14 shows a chemical composition comparison of steel S355J2G3 among Spain, Poland, Italy, Germany and Portugal with the European Standard EN 10025-2:2004.

In this table components as carbon, manganese, silicon, phosphorus and sulphur appears to be in every S355J2G3 steel. This leads us to think that this compounds seems to be crucial in looking for good quality chemical composition, even more chemical compounds are found in some of this steels.

	EN 10025-2:2004 [31]	Spain [37]	Poland [38]	Italy [39]	Germany [34]	Portugal [40]
C [max %]	0.2	0.17	0.14	0.193	0.222	0.1
Mn [max %]	1.6	1.235	0.88	1.520	1.580	0.64
Si [max %]	0.55	0.225	0.31	0.36	0.251	0.15
P [max %]	0.03	0.01	0.066	0.015	0.022	0.022
S [max %]	0.03	0.0006	0.027	0.0004	0.028	0.041
N [max %]	0.012	-	-	-	-	-
Cu [max %]	0.55	-	0.345	-	-	0.38
Al [max %]	-	0.032	-	0.026	0.039	-
Cr [max %]	-	0.072	-	-	-	0.076
Ni [max %]	-	0.058	-	-	0.04	0.095
Mo [max %]	-	0.016	-	-	-	0.014
Cev [max %]	0.47	-	-	-	-	-

Table 14. Chemical composition comparison of steel S355J2G3 in various countries.

As it was mentioned before, chemical composition varies due to the properties of the soil composition in each country. An appropriate chemical composition can provide excellent mechanical properties.

4.2.3 Fatigue properties

Knowledge of fatigue resistance of the material plays a key role during design and maintenance in civil engineering industry.

Steel S355 fatigue properties from specimens of various countries are included in the following chapters. As a commonly steel used in structures, owing to its great characteristics, several specimens from all over Europe are tested and used for experimental data.

4.2.3.1 *S-N* curves

The *S-N* curves approach is an established fatigue prediction technique used in many fields of applications. Common *S-N* curves are performed with $\Delta\sigma$-*N* or σ_a-*N* experimental data.

In S355 case, *S-N* curves found from the literature were plotted in $\Delta\sigma$-*N*, being $\Delta\sigma$ the stress amplitude and *N* the number of cycles in a logarithmic scale.

It should be noted that lots of articles of steel S355 from the literature were used for welded joints, which caused less specimens that met the requirements than expected.

Four specimens were finally used in order to compare their fatigue characteristics.

To begin with, first specimen used is a steel S355J0 from Czech Republic. **Figure 10** shows the geometry of the specimen used for *S-N* curves. The specimen has a cross-section area S_0 of 19.634 mm^2.

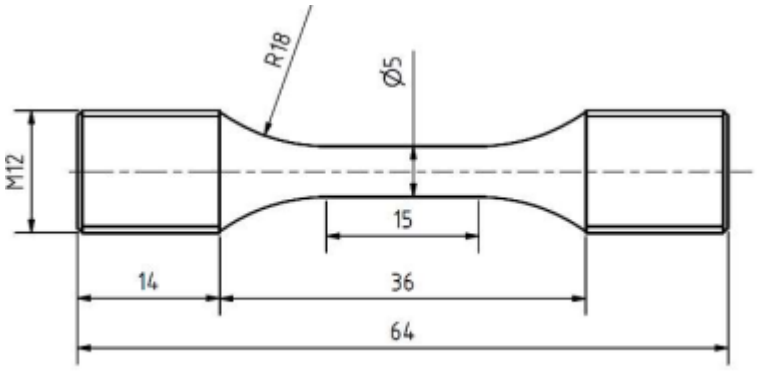

Figure 10. Geometry of smooth cylindrical specimen made of steel S355J0 from Czech Republic, retaken from [23]

The specimen was tested in a cyclic loading with a stress ratio R=0.1.

S-N curve of S355J0 steel was plotted in order to observe its fatigue behaviour and compare it with other specimens. As it was mentioned before, principles of Basquin's law were used to measure the specimen.

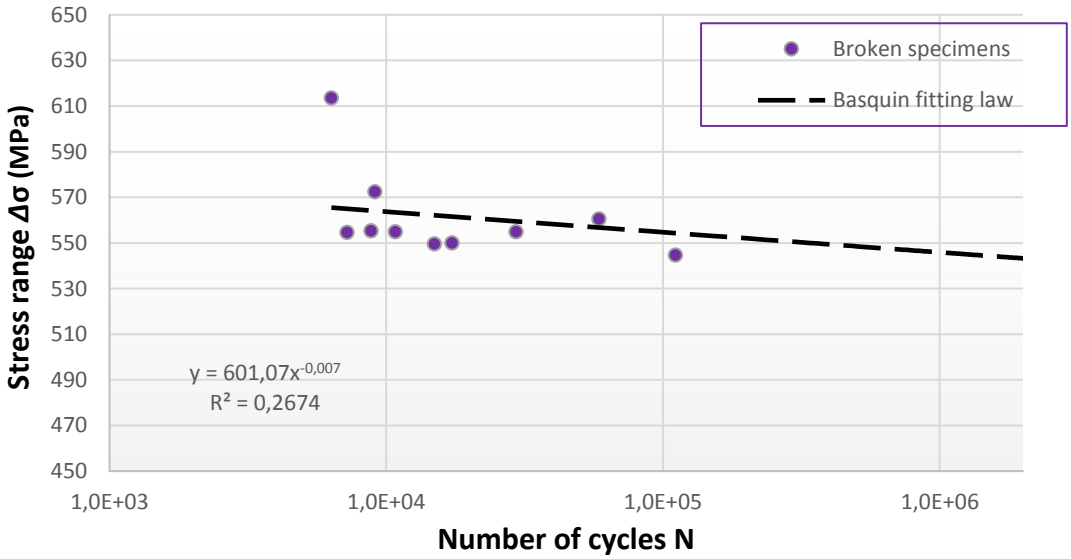

Graph 11. *S-N* curve of steel S355J0 from Czech Republic, data obtained from [23]

In **Table 10**, the results from the experimental data at high number of cycles are added.

Czech Republic [23]				
N **[cycles]**	**1.0E+04**	**1.0E+05**	**1.0E+06**	**1.0E+07**
$\Delta\sigma$ **[MPa]**	563.540	554.530	545.663	536.939
$\Delta\sigma/\sigma_u$ σ_u=550 MPa	1.02	1	0.99	0.97

Table 15. Stress evaluation at a High-Cycle Fatigue regime of S355J0 from Czech Republic.

No information about ultimate strength σ_u is available in the literature, but mean value of ultimate strength (σ_u= 550 MPa) was used in order to estimate the relationship

between $\Delta\sigma$ and σ_u. Nevertheless, *S-N* curve provides us information in which the specimens break practically at the same stress range value at a HCF regime, in which seems to have good fatigue strength properties.

The second specimen used is a steel S355 from Portugal. **Figure 11** shows the smooth geometry of the specimen used for experimental data and **Table 16** specifies the dimensions adopted for steel S355. The specimen has a cross-section area S_0 of 30 mm^2.

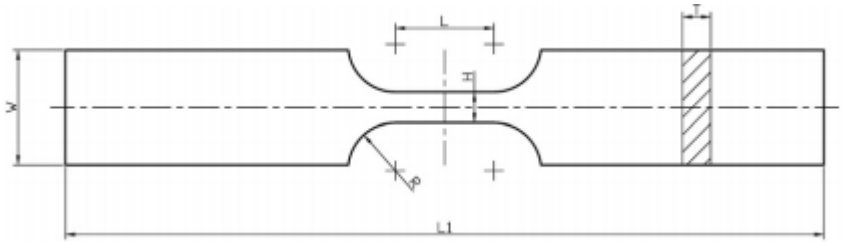

Figure 11. Geometry of smooth plane specimen made of steel S355 from Portugal, retaken from [36]

Specimen	W [mm]	T [mm]	L [mm]	L1 [mm]	H [mm]	R [mm]
S355	20	5	15	100	6	12

Table 16. Nominal dimension of smooth specimen made of steel S355 from Portugal; data obtained from [36]

The fatigue tests of the specimen were performed using cyclic loading with stress ratio *R*=0. Specimens were tested with a force up to 100 kN and a frequency that adjusted to results.

S-N curve from experimental data was plotted in order to analyse its fatigue behaviour and to compare it with other specimens. As in previous experiments, Basquin's law principles were used to measure the experimental data.

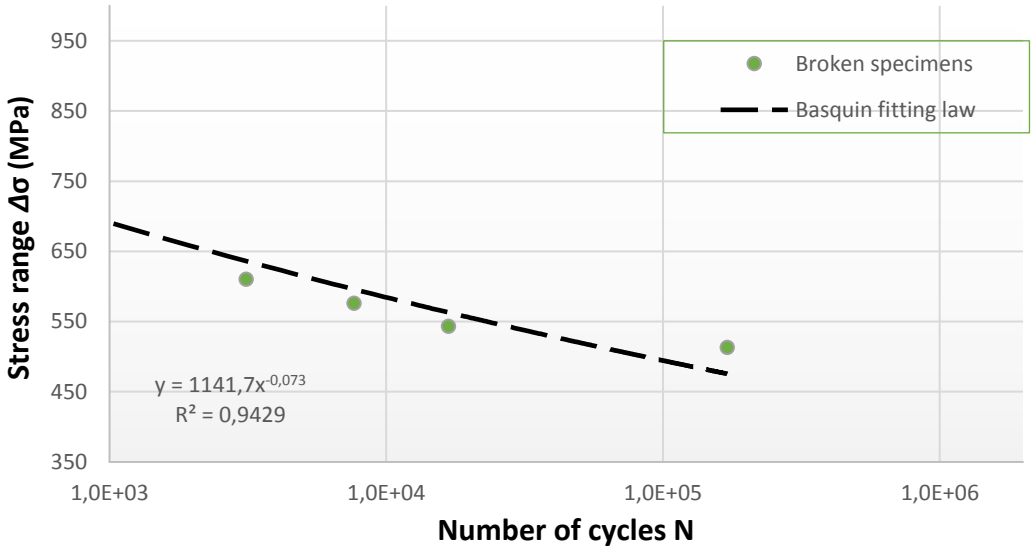

Graph 12. *S-N* curve of steel S355 from Portugal, data obtained from [36]

Table 17 shows the results of the *S-N* curve at high number of cycles.

Portugal [36]				
N **[cycles]**	**1.0E+04**	**1.0E+05**	**1.0E+06**	**1.0E+07**
$\Delta\sigma$ **[MPa]**	582.843	492.665	-	-
$\Delta\sigma/\sigma_u$ σ_u=550 MPa	1.05	0.89	-	-

Table 17. Stress evaluation at a High-Cycle Fatigue regime of S355 from Portugal.

No information about ultimate strength σ_u was obtained from the literature, but as it was explained before, mean value of ultimate strength (σ_u=550 MPa) was used in order to estimate the relationship between $\Delta\sigma$ and σ_u. Nevertheless, the *S-N* curve shows a typically descendant slope in which the stress range's resulting data at high number of cycles for broken specimens apparently shows good strength fatigue properties.

Third specimen used but not less important is a steel S355J2 from Germany. **Figure 12** shows the geometry of the smooth specimen used for experimental data. The specimen has a cross-section area S_0 of 960 mm^2.

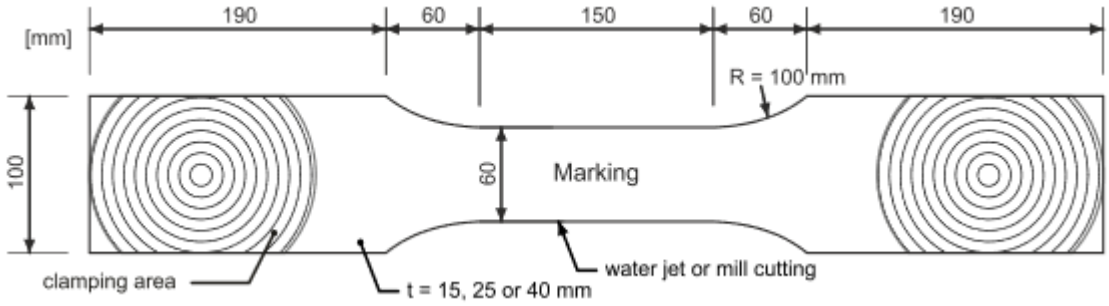

Figure 12. Geometry of smooth plane specimen made of steel S355 from Germany, retaken from [41]

For this experiment, thickness of 15 mm was used in order to try to adjust it with previous specimens. Also, the specimens were hard stamped in a defined area which do not affect their fatigue life.

Fatigue test of the specimen were performed using cyclic loading with a stress ratio *R*=0.1. Machines static capacities are of 1 MN and 1.6 MN. However, specimens with 15 mm of thickness were tested at 1 MN. Depending on the fatigue load, the test frequency varied from 5 to 9 Hz.

S-N curve of S355J2 steel was plotted in order to observe its fatigue behaviour and compare it with other specimens. As it was mentioned before, principles of Basquin's law were used to measure the specimen.

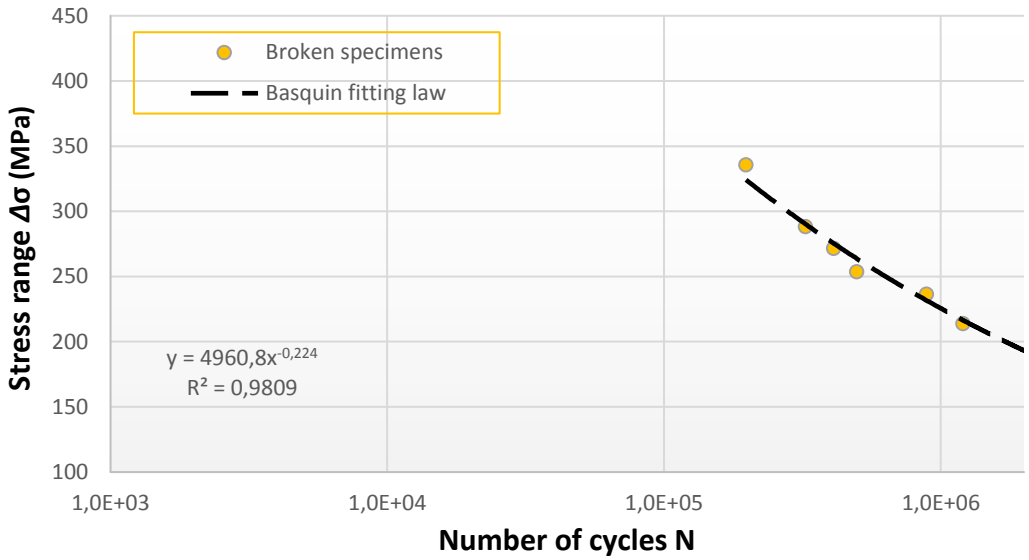

Graph 13. *S-N* curve of steel S355J2 from Germany, data obtained from [41]

Table 18 shows the results of the experimental data at high number of cycles.

Germany [41]				
N [cycles]	1.0E+04	1.0E+05	1.0E+06	1.0E+07
Δσ [MPa]	-	376.315	224.673	134.137
$\Delta\sigma / \sigma_u$ σ_u=550 MPa	-	0.68	0.41	0.24

Table 18. Stress evaluation at a High-Cycle Fatigue regime of S355J2 from Germany.

Unfortunately, no information about ultimate strength σ_u was included in the literature, but mean value of ultimate strength (σ_u= 550 MPa) was used in order to estimate the relationship between $\Delta\sigma$ and σ_u. However, *S-N* curves provided us some valid information. Fatigue strength of the specimens at LCF regimes seems to be high,

as none of the specimens broke before 1.0E+05 cycles. However, stress range at HCF regime starts to decrease very fast up to 1.0E+05 cycles, which seems to not have very good fatigue strength properties at HCF. One possible cause of this may be its cross-section area, as the specimen is much bigger than previous ones or due to its chemical composition.

Finally, fourth specimen is a steel S355 from Portugal. **Figure 13** shows the geometry for the smooth specimen used for *S-N* data and **Table 19** specifies the dimensions adopted for steel S355. The specimen has a cross-section area S_0 of 93.75 mm^2.

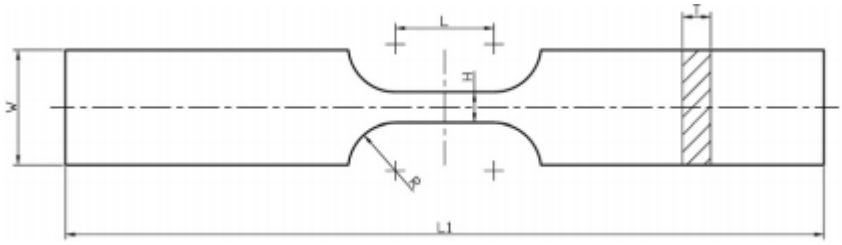

Figure 13. Geometry of smooth plane specimen made of steel S355 from Portugal, retaken from [40].

Specimen	W [mm]	T [mm]	L [mm]	L1 [mm]	H [mm]	R [mm]
S355	30	7.5	26	200	12.5	8

Table 19. Nominal dimension of smooth specimen made of S355 from Portugal, data obtained from [40]

The fatigue tests of the specimen were performed using cyclic loading with stress ratio *R*=-1. Specimens were tested with a force up to 100 kN and a frequency that adjusted to results.

S-N curve from experimental data was plotted in order to analyse its fatigue behaviour and to compare it with other specimens. As in previous experiments, Basquin's law principles were used to measure the experimental data.

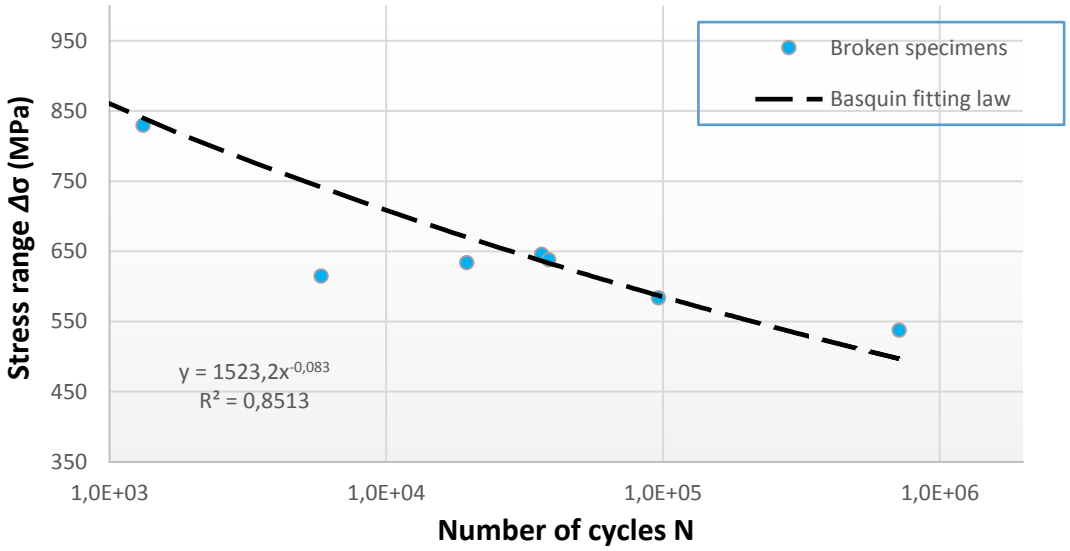

Graph 14. *S-N* curve of steel S355 from Portugal, data obtained from [40]

In **Table 20**, the results of the experimental data at high number of cycles are shown.

Portugal [40]				
N [cycles]	**1.0E+04**	**1.0E+05**	**1.0E+06**	**1.0E+07**
Δσ [MPa]	709.180	585.810	-	-
$\Delta\sigma/\sigma_u$ σ_u=550 MPa	1.28	1.06	-	-

Table 20. Stress evaluation at a High-Cycle Fatigue regime of S355 from Portugal.

Unfortunately, as in previous S355 specimens, no information of ultimate strength σ_u was available in the literature, but as it was explained before, mean value of ultimate strength (σ_u=550 MPa) was used in order to estimate the relationship between $\Delta\sigma$ and σ_u. But nevertheless, *S-N* curve provided us some valid information. First to notice is that at HCF regime, specimens broke at a "similar" high stress range values, which seems to have very good fatigue strength properties. Finally, a descendant slope with low inclination and the stress range values leads us to think that is a common *S-N* curve for a S355 steel.

Fatigue life prediction of specimens seems to be impossible to define with certainty, but this experiments helps us to understand when the specimens fatigue life ends.

4.2.3.2 *S-N* curves comparison

In first place, an essential factor to compare various specimens is the stress ratio *R*. It is crucial that the specimens have to be loaded with the same type of cycle; if not, fatigue crack may propagate in another way, since tension and compression stresses are completely different.

With this information, the only specimens that have the same stress ratio *R* are the S355J0 from Czech Republic and the S355J2 from Germany.

Comparison of experimental data shows that *S-N* curves of both steel grades, presented in **Graph 15** differ a lot.

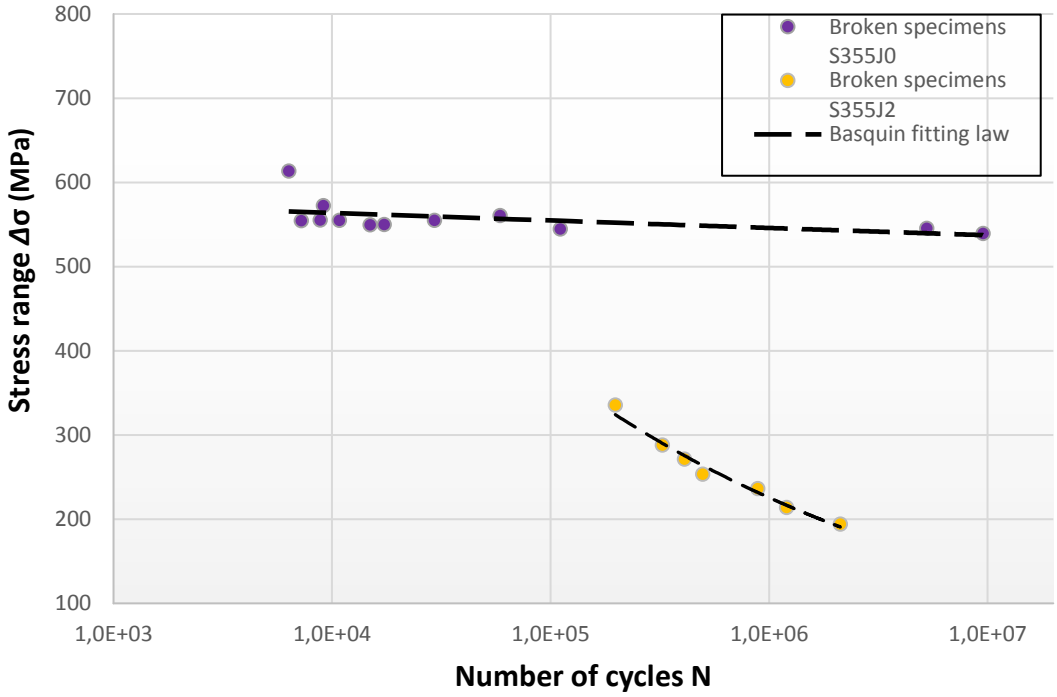

Graph 15. *S-N* curve comparison between S355J0 from Czech Republic [23] and S355J2 from Germany [34] (*R*=0.1).

Nevertheless, no more *S-N* curve comparison has been possible, since even various steels as both S355 from Portugal have the same geometry, one of them is loaded at stress ratio (*R*=0) and the other one at (*R*=-1), which makes impossible their comparison.

4.2.3.3 Crack propagation curve

In this part, comparison of the fatigue crack growth resistance of S355J0 and S355J2 steel grades is shown. Data from those steels was obtained from experimental tests of compact tension (*CT*) specimens.

The tested *CT* specimens had dimensions:

L [mm]	W [mm]	B [mm]	a_n [mm]	H/2 [mm]	β_1
62.5	50	10	12.5	30	60°

Table 21. *CT* specimen dimensions for S355J0 and S355J2 steel grades [42]

Two rolling directions A and B (rotated by 90º) were used in order to see the influence of the material structure orientation on the crack propagation rate. **Figure 14** shows the specimen orientation in the metal sheet, in which specimens marked with letter "A", the initial crack is orientated parallel to the rolling direction.

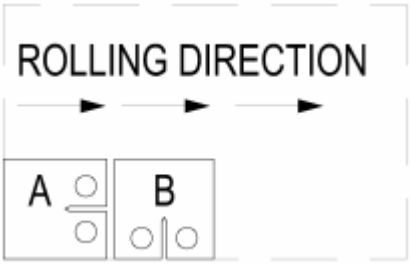

Figure 14. *CT* specimen rolling direction, retaken from [42]

The fatigue crack growth rate experiments were measured from a computer-controlled testing machine with a force up to 20 kN. Tests were conducted under load control. A stress ratio R=0.1 for the load cycle and a frequency varying from 96 (for the shortest cracks) to 42 Hz (for the longest cracks).

In **Graph 16**, the comparison of the experimental data from S355J0 and S355J2 in both rolling directions in the Paris region is shown.

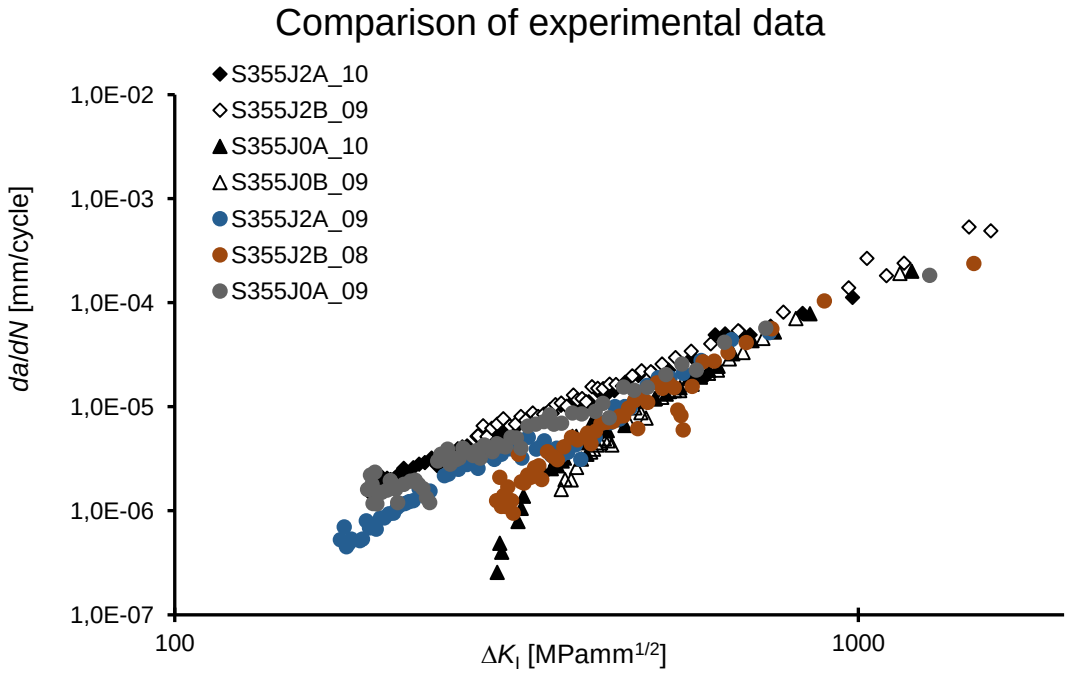

Graph 16. Experimental results of S355J0 and S355J2 crack propagation rate, data adopted from [42]

In this graph we can observe that both's S355J0 and S355J2 crack growth rates are very similar. At the same time, rolling direction does not seems to affect in the crack growth rate in Paris region as well.

The difference in the crack growth rates between the tested specimens could be resulting from the different amount of particles in the material structure and their influence on the crack growth mechanism.

The material constants C and m were estimated from the experimental data measured in Paris region. The results are given in Table 22, together with the data from Jesus et al. [40] and Adedipe et al. [43].

Material	C [mm/cycle·MPa·$mm^{0.5}$]	m [-]
S355J2A	2.00E-12	2.595
S355J2B	1.00E-12	2.711
Adedipe S355J2 [43]	3.00E-14	3.296
S355J0A	2.00E-15	3.605
S355J0B	2.00E-15	3.638
De Jesús S355 [40]	3.00E-15	3.561

Table 22. Comparison of material constants C and m from experimental measurement and literature, data of S355J0 and S355J2 obtained from [42]

Conclusion

In thesis, static and fatigue properties of two structural steels S235 and S355 from various countries of the European Union have been analysed and compared from experimental and literature data.

From the static point of view, chemical composition, mechanical properties and strength properties were used in this comparison.

From the fatigue point of view, *S-N* curves approach (Wöhler curves) and Fracture Mechanics approach (Crack Propagation Rate Curve) were used in this comparison.

The following conclusions can be drawn:

- Most of the literature from S235 and S355 structural steels are focused on the fatigue properties of welds/welded joints.
- Not much information from S235 structural steel can be found in the literature.
- Biggest variances in monotonic properties of steel from various countries are found in steel S355J2G3.
- Variances in chemical composition seems to be produced by the soil composition of each country.
- *S-N* curve comparison cannot be compared if stress ratio *R* has not the same value, as different stress distribution in the specimen is produced due to different load cycles.
- Fatigue strength characteristics of steels may be related with variances in the microstructure of the material.
- Static properties, specifically chemical composition appears to be key in fatigue behaviour of the materials.
- Rolling direction in crack propagation rate curves seems to not be important.
- The S355J2 steel grade shows higher crack growth rates when compared with S355J0.
- S355J2 steel grade shows a greater fatigue-endurance limit.

References

[1] Hotel Intriago. (25/04/2019). Puente romano Cangas de Onís. Retaken from https://hotelintriago.com/monumentos/puente-romano-cangas-de-onis/

[2] Diario del viajero. (25/04/2019). Asturias, horeos y cabazos. Retaken from https://www.diariodelviajero.com/espana/asturias-horreos-paneras-y-cabazos

[3] Oviedocongresos. (25/04/2019). Palacio de Exposiciones y Congresos ciudad de Oviedo. Retaken from http://oviedocongresos.com/portfolio/palacio-de-congresos-ciudad-de-oviedo/

[4] WIRSCHING, Paul H. Statistical summaries of fatigue data for design purposes. 1983.

[5] Albert, W. A. J. (1838) "Über Treibseile am Harz" *Archiv für Mineralogie Geognosie Bergbau und Hüttenkunde*, vol. 10, pp 215-34

[6] *Wöhler, A. (1870). "Über die Festigkeitsversuche mit Eisen und Stahl". Zeitschrift für Bauwesen.* ***20****: 73–106.*

[7] *Basquin, O. H. (1910). "The exponential law of endurance test". Proceedings of the American Society for Testing and Materials.* ***10****: 625–630.*

[8] *K.B. Broberg (1997). H.P. Rossmanith (ed.). Fracture Research in Retrospect: An anniversary volume in honour of G.R. Irwin's 90th birthday. CRC Press. p. 142. ISBN 9054106794.*

[9] *EN 10027, European committee for standardisation.*

[10] EN 10025-2:2004

[11] DAVIS, Joseph R. (ed.). *Tensile testing*. ASM international, 2004.

[12] Southern Inspection and Testing. (1/05/2019). Tensile Testing. Retaken from http://www.southerninspection.com/PageDisplay.asp?p1=13507

[13] Engineering Archives. (1/05/2019). Tensile Test. Retaken from http://www.engineeringarchives.com/les_mom_tensiletest.html

[14] *Davis, Joseph R. (2004). Tensile testing (2nd ed.). ASM International.*

[15] Yun, Xiang & Gardner, Leroy. (2017). Stress-strain curves for hot-rolled steels. Journal of Constructional Steel Research. 133. 36-46. 10.1016/j.jcsr.2017.01.024.

[16] ROYLANCE, David. Stress-strain curves. Massachusetts Institute of Technology study, Cambridge, 2001.

[17] ESDEP WG 2 APPLIED METALLURGY. (2/05/2019). Lecture 2.3.1 Introduction to the Engineering Properties of Steels. Retaken from http://fgg-web.fgg.uni-lj.si/~/pmoze/esdep/master/wg02/l0310.htm

[18] Cyclic deformation and strain life (ε-N) approach. (2/05/2019). Monotonic tension test and stress-strain behaviour. Retaken from https://www.efatigue.com/training/Chapter_5.pdf

[19] Raymond Kwesi Nutor, Nana Kwabena Adomako, Y. Z. Fang, Using the Hollomon Model to Predict Strain-Hardening in Metals, *American Journal of Materials Synthesis and Processing*. Vol. 2, No. 1, 2017, pp. 1-4. doi: 10.11648/j.ajmsp.20170201.11

[20] ASM Handbook, Volume 1:Properties and Selection:Irons,Steels, and High-Performance Alloys ASM Handbook Committee, p673-688

[21] Materiales aeronáuticos. (4/05/2019). Fatiga. Retaken from http://www.aero.ing.unlp.edu.ar/catedras/archivos/Fatiga.pdf

[22] Vassilopoulos, A. P. (2015). *Fatigue and Fracture of Adhesively-Bonded Composite Joints - Behaviour, Simulation and Modelling - 4.4 Fatigue Characterization by the S-N Approach.* Elsevier.

[23] SEITL, Stanislav, et al. Evaluation of fatigue properties of S355 J0 steel using ProFatigue and ProPagation software. *Procedia Structural Integrity*, 2018, vol. 13, p. 1494-1501.

[24] Ferguson, George Thambyah, Ashvin Hodgson, Michael A. Wade, Kelly. (2011). *Structural Integrity and Failure - 9.1 Introduction.* Trans Tech Publications Ltd.

[25] Oberg, Erik Jones, Franklin D. Horton, Holbrook L. Ryffel, Henry H.. (2016). *Machinery's Handbook (30th Edition) - 10.1.8 The Influence of Mean Stress on Fatigue.*

[26] Frost, N.E. Marsh, K.J. Pook, L.P.. (1974). *Metal Fatigue - 5.2.1 Modes of Crack Growth.* Dover Publications.

[27] Compact tension test. (7/05/2019). Retaken from https://en.wikipedia.org/wiki/Compact_tension_specimen#cite_ref-bower_3-0

[28] Bai, Yong. (2003). *Marine Structural Design - 16.6 Fracture Mechanics in Fatigue Analysis.* Elsevier.

[29] Lee, Yung-Li Pan, Jwo Hathaway, Richard B. Barkey, Mark E. (2005). *Fatigue Testing and Analysis - Theory and Practice - 6.6.3 Walker Equation.* Elsevier.

[30] Mesteel. (8/05/2019). Equivalents of Carbon Steel Qualities. Retaken from https://www.mesteel.com/qualities/equivalentscs.htm

[31] *EN 10025-2:2004* Hot rolled products of structural steels – Part2: Technical delivery conditions for non-alloy structural steels.

[32] ROBAKOWSKI, T.; CZUCHRYJ, J. The effect of overloading on the strength of St3W steel welded joints. *Welding International*, 1990, vol. 4, no 6, p. 425-429.

[33] BAYRAKTAR, E.; KAPLAN, D.; YILBAS, B. S. Comparative study: Mechanical and metallurgical aspects of tailored welded blanks (TWBs). *Journal of materials processing technology*, 2008, vol. 204, no 1-3, p. 440-450.

[34] HAN, Seungho, et al. Fatigue crack propagation near fatigue threshold in various structural steels. *Steel research*, 1996, vol. 67, no 12, p. 549-554.

[35] SŁOWIK, Jacek; ŁAGODA, Tadeusz. The fatigue life estimation of elements with circumferential notch under uniaxial state of loading. *International Journal of Fatigue*, 2011, vol. 33, no 9, p. 1304-1312.

[36] CARVALHO, D., et al. FATIGUE BEHAVIOUR OF STRUCTURAL STEELS. COMPARISON OF STRAIN-LIFE AND FATIGUE CRACK PROPAGATION DATA COMPORTAMENTO À FADIGA DE AÇOS ESTRUTURAIS. RELAÇÕES DEFORMAÇÃO-VIDA E TAXAS DE PROPAGAÇÃO DE FENDAS DE FADIGA.

[37] Estudio Experimental y Evaluación de Modelos de Plano Crítico en Fatiga Biaxial-Final Bachelor Thesis Ángel Rodríguez Ruiz.

[38] ROZUMEK, Dariusz; MACHA, Ewald. Opis rozwoju pęknięć zmęczeniowych w materiałach sprężysto-plastycznych przy proporcjonalnym zginaniu ze skręcaniem. Oficyna Wydawnicza Politechniki Opolskiej, 2006.

[39] CHIARELLI, M.; LANCIOTTI, Agostino; SACCHI, M. Effect of plasma cutting on the fatigue resistance of Fe510 D1 steel. *Journal of engineering materials and technology*, 2000, vol. 122, no 1, p. 141-145.

[40] DE JESUS, Abílio MP, et al. A comparison of the fatigue behavior between S355 and S690 steel grades. *Journal of Constructional Steel Research*, 2012, vol. 79, p. 140-150.

[41] STRANGHÖNER, Natalie; JUNGBLUTH, Dominik. Fatigue strength of marked steel components. *Procedia Engineering*, 2015, vol. 133, p. 282-293.

[42] SEITL, Stanislav, et al. Comparison of the fatigue crack propagation rates in S355 J0 and S355 J2 steel grades. En *Key Engineering Materials*. Trans Tech Publications, 2018. p. 91-96.

[43] ADEDIPE, Oyewole; BRENNAN, Feargal; KOLIOS, Athanasios. Review of corrosion fatigue in offshore structures: Present status and challenges in the offshore wind sector. *Renewable and Sustainable Energy Reviews*, 2016, vol. 61, p. 141-154.

List of Abbreviations

JIS	Japanese International Standard
DIN	German Standard
GB	Chinese Standard
ISO	International Organization of Standardization
VLCF	Very Low-Cycle Fatigue
LCF	Low-Cycle Fatigue
HCF	High-Cycle Fatigue
VHCF	Very High-Cycle Fatigue
ASTM	American Society of Testing and Materials

List of Symbols

σ_y	Yield strength
σ_u	Ultimate strength
E	Modulus of elasticity
A	Elongation
L_0	Gage length
S_0	Cross-section area
υ	Poisson's ratio
F	Force
ε	Strain
σ or S	Stress
N	Number of cycles
K	Strength coefficient
n	Strain-hardening exponent
α	Characteristic property of the material
σ_m	Mean stress
σ_a	Stress amplitude
$\Delta\sigma$	Stress range
R	Stress ratio
A, B	Material constants of Basquin's model
N_f	Number of cycles to failure
a	Crack length
a_0	Initial crack length
a_f	Final crack length
CT	Compact tension
ΔK	Stress intensity factor range
ΔK_{th}	Threshold stress intensity factor range
Y	Funciton depending on geometrics and loading conditions
da	Increment of crack length
dN	Increment of lifetime as number of cycles
C, m	Paris' law constants

List of Figures

List of Graphs

List of Tables

BRNO UNIVERSITY OF TECHNOLOGY

FACULTY OF CIVIL ENGINEERING

PROPIEDADES DEL ACERO APLICADO EN LA INDUSTRIA DE LA INGENIERÍA CIVIL EN DETERMINADOS PAÍSES:S235 Y S355

BACHELOR THESIS

AUTOR Ignacio Rodríguez Sánchez

SUPERVISOR Assoc. Prof. Stanislav Seitl
SUPERVISOR SPECIALISTA: Ing. Petr Miarka

BRNO 2019

RESUMEN

Esta tesis está enfocada en la comparación de las propiedades de los aceros S235 y S355 en varios países de Europa. De esta manera, se ha realizado una comparación entre su composición química, propiedades mecánicas y sus propiedades a fatiga como son las curvas *S-N* (curvas de Wöhler) y las velocidades de propagación de grietas.

Estos dos tipos de aceros han sido comparados con el objetivo de estudiar la influencia del material en las propiedades a fatiga de éstos.

La información usada en este proyecto fue obtenida en base a publicaciones de diferentes artículos sobre estos tipos de aceros y de un programa experimental realizado en el Institute of Physics of Materials ASCR en cooperación con la Facultad de Ingeniería Civil de Brno University of Technology.

PALABRAS CLAVES

Acero, S235, S355, propiedades mecánicas, composición química, resistencia del material, propiedades a fatiga, curvas S-N, velocidades de propagación de grietas.

CITA BIBLIOGRÁFICA

Ignacio Rodríguez Sánchez Propiedades del acero aplicado en la industria de la ingeniería civil en determinados países: S235 y S355. Brno, 2019. 26 p., 0 p. de archivos adjuntos. Trabajo de Fin de Grado. Brno Univeristy of Technology, Faculty of civil engineering y Universidad de Oviedo, Supervisor: Assoc. Prof. Stanislav Seitl. Supervisor especialista: Ing. Petr Miarka.

AGRADECIMIENTOS

Este Trabajo de Fin de Grado ha sido realizado bajo el apoyo del programa ERASMUS Plus y en colaboración con el Czech Science Foundation con contrato No. 17-01589S. Este programa ha sido realizado bajo el "National Sustainability Programme I" y proyecto "AdMaS UP-Advanced Materials, Structures and Technologies" (No.LO1408) apoyado por el Ministro de Educación, Juventud y Deportes de la República Checa.

Me gustaría agradecer la ayuda aportada por mis tutores en Brno Stanislav Seitl y Petr Miarka, así como a mi tutora en Gijón María Jesús Lamela, quienes hicieron posible que pudiera realizar este trabajo. De la misma manera querría agradecer a mi familia, que sin ninguna duda sin su apoyo y ayuda no hubiera sido capaz de llevarlo a cabo.

Índice

1. Introducción

La importancia del material en la industria de la ingeniería civil ha sido crucial en los últimos cientos de años, e incluso actualmente sigue siendo unos de los factores más influyentes y que marcan más la diferencia en este sector.

La demanda del acero como material de construcción se encuentra en un nivel creciente en esta industria. La gran resistencia del acero, así como su ductilidad, adaptación a prefabricación, etc., ha sido siempre un factor muy positivo para convertirse en uno de los materiales más importantes a la hora de escogerlo como tipo de material en la estructura que se quiere construir.

Una de las propiedades más importantes del acero son la tensión de fluencia (σ_y), la tensión de rotura (σ_u), el módulo de Young (E), la elongación ($A\%$) y la composición química.

Sin embargo, aunque tiene muchas ventajas también tiene sus defectos. Aquí es donde la fatiga aparece. En general, la fatiga es quizás el factor de fallo más importante a tener en cuenta en el ámbito del diseño estructural y mecánico. Para algún tipo de producto, la fatiga ocurre para más del 80% de los casos observados en fallos de servicio.

Su importancia reside en que la fractura de materiales por fatiga ocurre a veces de una manera catastrófica y sin previo aviso causando un severo daño estructural y pérdida de vida del material. La realización de un buen diseño para evitar este tipo de procesos de rotura por fatiga es complicada, dado que los estreses a menudo se producen por procesos aleatorios.[1]

2. Objetivo

El objetivo de este Trabajo de Fin de Grado es obtener información sobre las propiedades de los aceros S235 y S355 en varios países de la Unión Europea y compararlos entre ellos con el propósito de entender sus propiedades a fatiga.

Con este fin, las propiedades mecánicas, como pueden ser la composición química y las propiedades estáticas serán medidas de aceros S235 y S355 sobre probetas lisas para compararlos entre ellos y con los estándares dados por la Unión Europea (EN100025-2:2004).

A su vez, las curvas *S-N* y las curvas de propagación de grietas de los aceros S235 y S355 de los países seleccionados han sido evaluadas a través de las curvas de Wöhler con objeto de comparar la influencia del material en sus propiedades a fatiga.

3. Materiales seleccionados usados en el área de la industria civil

En los siguientes apartados de este trabajo, la atención se ha realizado en los aceros S235 y S355, en donde se ha realizado un pequeño estudio de sus propiedades estáticas y a fatiga.

3.1 *Acero S235*

El acero S235 es un acero estructural que cumple con los estándares europeos EN 10025-2:2004. Es un acero carbonado que puede ser empleado en un amplio rango de procesos, ya sea en la industria mecánica o en edificios y puentes.

Una de las principales características de este acero es su tensión de fluencia de 235 MPa para espesores no superiores a 16 mm, pudiendo disminuir a medida que aumenta este último.

En la **Tabla 1** se puede observar la designación de este acero en varios países:

Acero S235J2G3 [2]							
EN 10025-2	España	Polonia	Italia	Alemania	Portugal	U. K.	China
1.0116	AE 235 D	St3w	Fe 360 D	St 37-3N	Fe 360 D	40D	Q 235D

***Tabla 1**. Designación del acero S235J2G3 en varios países.*

Las propiedades mecánicas de los aceros estructurales son fundamentales para su clasificación y aplicación en la industria.

En la **Tabla 2** se puede observar los diferentes valores de la tensión de fluencia (σ_y), tensión de rotura (σ_u), módulo de Young (*E*) y elongación (*A%*) de varios aceros S235J2G3 de Europa comparados con los estándares EN 10025-2:2004:

	EN 10025-2:2004 [3]	Polonia [4][4]	Italia [5]	Alemania [6]
Min σy [MPa]	235	307	282	277
σu [MPa]	360/510	461	412	415
E [GPa]	-	207	-	-
A [%]	-	33.8	37	43

***Tabla 2**. Comparación de las propiedades monotónicas del acero S235J2G3 en varios países.*

De la misma manera, la **Tabla 3** presenta las composiciones químicas de varios países de Europa comparados con los estándares EN 10025-2:2004:

	EN 10025-2:2004 [3]	Polonia [4]	Italia [5]	Alemania [6]
C [max %]	0.17	0.16	0.164	0.084
Mn [max %]	1.5	0.81	0.397	0.658
Si [max %]	-	0.22	0.018	0.169
P [max %]	0.025	0.01	0.012	0.02
S [max %]	0.025	0.02	0.008	0.009
N [max %]	-	-	0.0033	-
Cu [max %]	0.55	-	-	-
Al [max %]	-	0.04	0.035	0.039
Cr [max %]	-	0.13	-	0.03
Ni [max %]	-	0.09	-	0.035
Mo [max %]	-	-	-	-
Cev [max %]	0.4	-	-	-

***Tabla 3**. Comparación de la composición química del acero S235J2G3 en varios países.*

3.1.1 *Propiedades a fatiga*

Es bien conocido tanto en la industria mecánica como civil que la fatiga tiene un rol clave en el diseño y mantenimiento de las estructuras y máquinas. En este apartado se ha comparado las propiedades a fatiga mediante el uso de las curvas *S-N.*

Es importante remarcar que el acero S235 es menos usado que otros muchos en la industria, por lo que no se ha podido obtener mucha información. En este caso, las curvas fueron realizadas en σ_a-*N,* siendo σ_a la tensión alterna y *N* el número de ciclos.

El primer acero utilizado es un S235JR de Polonia. La **Figura 1** muestra la geometría de la probeta usado en los tests:

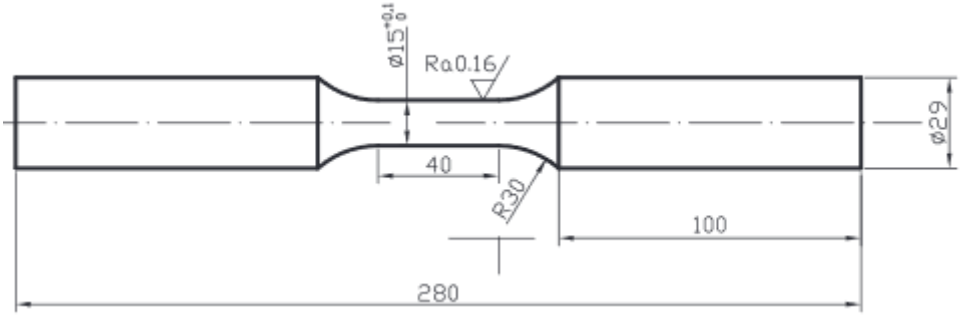

***Figura 1**. Geometría de la probeta cilíndrica hecha de acero S235 de Polonia, obtenida de [7]*

Posee un área en la sección transversal S_0 = 176.71 mm^2. A su vez, el ensayo a fatiga ha sido realizado con cargas cíclicas y un ratio (R=-1), una fuerza de 400 kN y una frecuencia de 5Hz.

El siguiente gráfico presenta la curva *S-N* de la probeta:

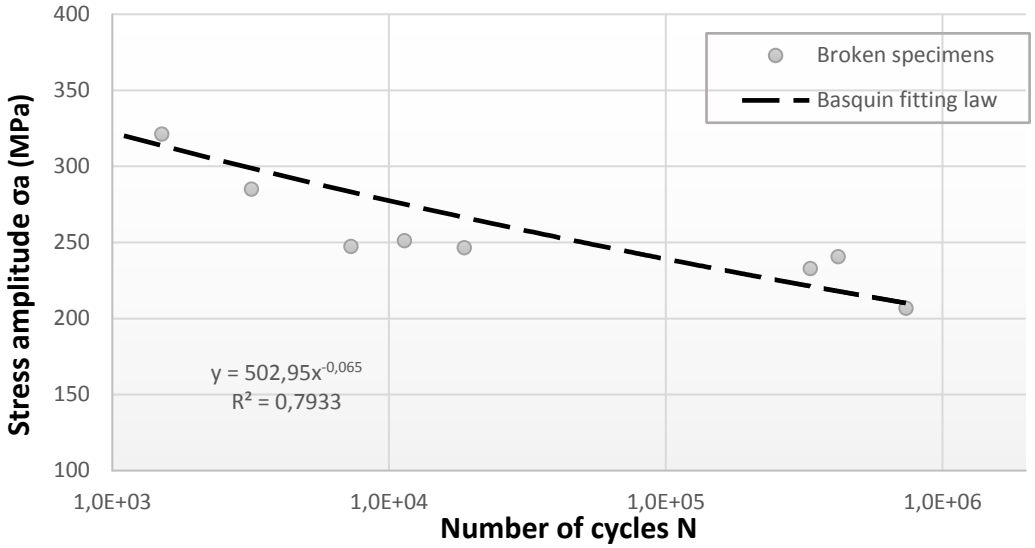

***Gráfico 1**. Curva S-N del acero S235JR de Polonia, información cogida de [7]*

La **Tabla 4** muestra los resultados del experimento a fatiga a altos ciclos.

Polonia [7]				
N [ciclos]	1.0E+04	1.0E+05	1.0E+06	1.0E+07
σ_a [MPa]	276.391	237.97	-	-
σ_a/σ_u σ_u =423 [MPa]	0.653	0.562	-	-

***Tabla 4**. Evaluación de la tensión a alto número de ciclos del acero S235 JR de Polonia.*

El segundo acero comparado en el experimento es un S235 de Portugal. La **Figura 2** muestra la geometría de la probeta utilizada en los tests y la **Tabla 5** especifica las dimensiones de la misma. El espécimen presenta una sección transversal S_0 de 30 mm^2.

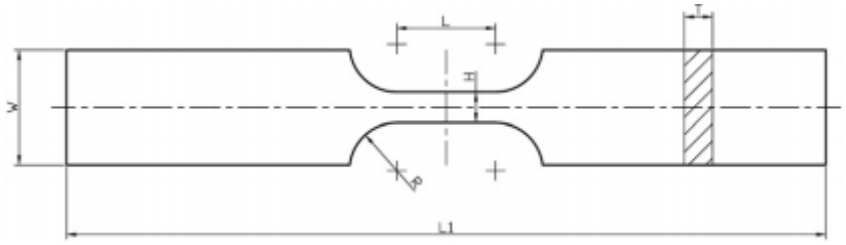

***Figura 2**. Geometría de la probeta plana hecha de acero S235 de Portugal, obtenido de [8]*

Probeta	W [mm]	T [mm]	L [mm]	L1 [mm]	H [mm]	R [mm]
S235	20	5	15	135	6	12

***Tabla 5**. Dimensiones de la probeta hecha de acero S235 de Portugal, información obtenida de [8]*

Los tests a fatiga fueron realizados con cargas cíclicas y un ratio (*R*=0). Las probetas fueron usadas con una fuerza hasta 100 kN y una frecuencia que se ajustaba a los resultados.

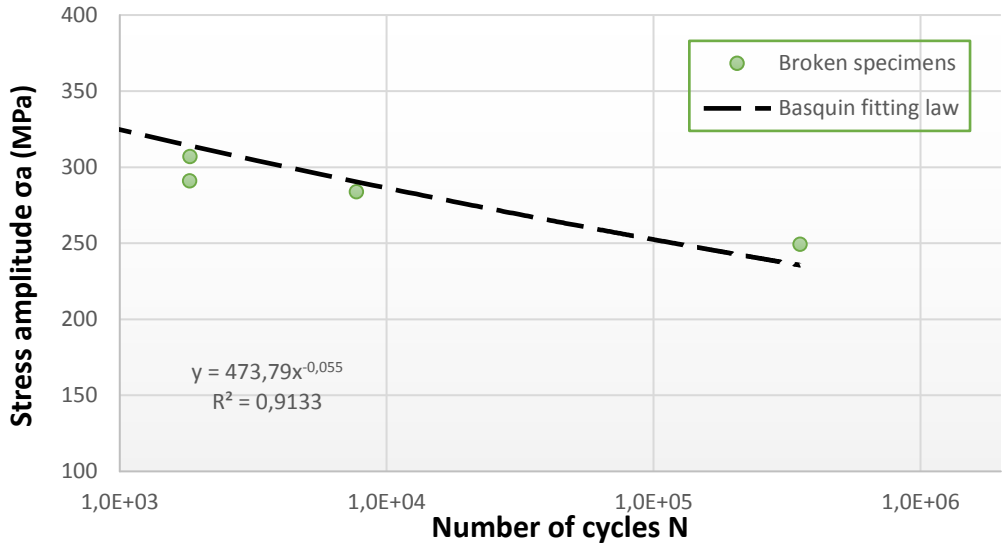

***Gráfico 2**. Curva S-N del acero S235 de Portugal, información obtenida de [8]*

La **Tabla 6** muestra los resultados a fatiga a altos ciclos.

Portugal [8]				
N **[ciclos]**	**1.0E+04**	**1.0E+05**	**1.0E+06**	**1.0E+07**
σ_a **[MPa]**	324.030	285.486	-	-
σ_a/σ_u σ_u=435 [MPa]	0.578	0.509	-	-

***Tabla 6**. Evaluación de la tensión a altos números de ciclos del acero S235 de Portugal.*

3.1.2 *Comparación de las curvas S-N de las probetas seleccionadas*

La comparación entre los aceros S235JR de Polonia y S235 de Portugal no ha sido posible debido a varios factores.

En primer lugar, el factor más esencial e importante, el ratio *R*. Es imprescindible que las probetas estén aplicadas con el mismo tipo de cargas cíclicas; ya que, si no, la grieta a fatiga puede propagarse de una manera totalmente distinta debido a que las tensiones de compresión y tracción son totalmente diferentes.

Finalmente, la geometría de las mismas era diferente.

3.2 *Acero S355*

El acero S355 es un acero estructural que cumple con los estándares de la Unión Europea EN 10025-2:2004. Este tipo de acero es utilizado en prácticamente cualquier faceta de la fabricación industrial.

Las principales características de este acero es su tensión de fluencia (σ_y) de 355 MPa a un espesor no superior a 16 mm, tendiendo a descender a medida que aumenta éste.

En la siguiente tabla podemos observar los diferentes nombres de este acero en varios países:

Acero S355J2G3 [2]							
EN 10025-2:2004	España	Poonia	Italia	Alemania	Portugal	U. K.	China
1.0570	AE 355 D	10HNAP	Fe 510 D	St 52-3N	Fe 510 D	50D	-

***Tabla 7**. Designación del acero S355J2G3 en varios países, información obtenida de [2]*

Las propiedades mecánicas de los aceros estructurales son fundamentales para su clasificación y aplicación en la industria. Este acero, al ser tan utilizado en la industria ha permitido obtener más información que el S235.

En la Tabla 8 se puede observar los diferentes valores de la tensión de fluencia (σ_y), tensión de rotura (σ_u), módulo de Young (*E*) y elongación (*A%*) de varios aceros S235J2G3 de Europa comparados con los estándares EN 10025-2:2004:

	EN 10025-2:2004 [3]	España [9]	Polonia [10]	Italia [11]	Alemania [6]	Portugal [12]
Min σ_y [MPa]	355	386	418	455	362	419
σ_u [MPa]	470/630	689	566	620	566	732
E [GPa]	-	206	215	-	206	-

***Tabla 8**. Comparación de las propiedades monotónicas del acero S355J2G3 en varios países.*

De la misma manera, la Tabla 9 presenta las composiciones químicas de varios aceros S355J2G3 de varios países:

	EN 10025-2:2004 [3]	España [9]	Polonia [10]	Italia [11]	Alemania [6]	Portugal [12]
C [max %]	0.2	0.17	0.14	0.193	0.222	0.1
Mn [max %]	1.6	1.235	0.88	1.520	1.580	0.64
Si [max %]	0.55	0.225	0.31	0.36	0.251	0.15
P [max %]	0.03	0.01	0.066	0.015	0.022	0.022
S [max %]	0.03	0.0006	0.027	0.0004	0.028	0.041
N [max %]	0.012	-	-	-	-	-
Cu [max %]	0.55	-	0.345	-	-	0.38
Al [max %]	-	0.032	-	0.026	0.039	-
Cr [max %]	-	0.072	-	-	-	0.076
Ni [max %]	-	0.058	-	-	0.04	0.095
Mo [max %]	-	0.016	-	-	-	0.014
Cev [max %]	0.47	-	-	-	-	-

***Tabla 9**. Comparación de la composición química del acero S355J2G3 en varios países.*

3.2.1 *Propiedades a fatiga*

Es bien conocido tanto en la industria mecánica como civil que la fatiga tiene un rol clave en el diseño y mantenimiento de las estructuras y máquinas. En este apartado se ha comparado las propiedades a fatiga mediante el uso de las curvas *S-N.*

Es importante remarcar que el acero S355 es más usado que otros muchos en la industria, por lo que se ha podido obtener más información. En este caso, las curvas fueron realizadas en $\Delta\sigma$-*N,* siendo $\Delta\sigma$ la amplitud de tensión y *N* el número de ciclos.

Cuatro probetas fueron usadas con el objetivo de obtener comparar las propiedades a fatiga.

Para comenzar, la primera probeta utilizada ha sido un acero S355J0 de la República Checa. La **Figura 3** muestra la geometría de la misma utilizada en los ensayos. El espécimen presenta una sección transversal S_0 de 19.634 mm^2.

La probeta ha sido ensayada con cargas cíclicas de ratio *R*= 0.1.

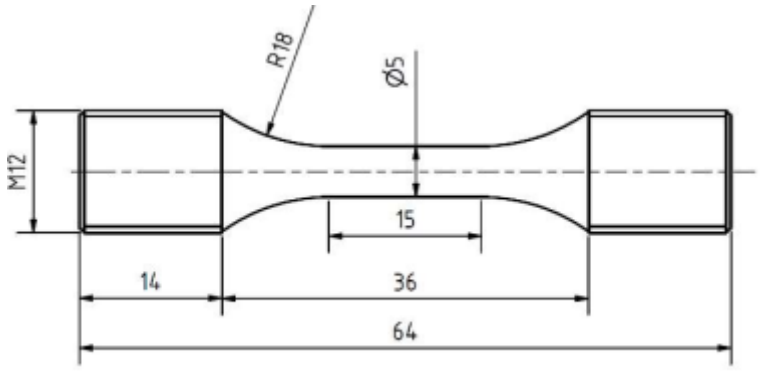

***Figura 3**. Geometría de la probeta cilíndrica hecha de acero S355J0 de la República Checa, obtenida de [13]*

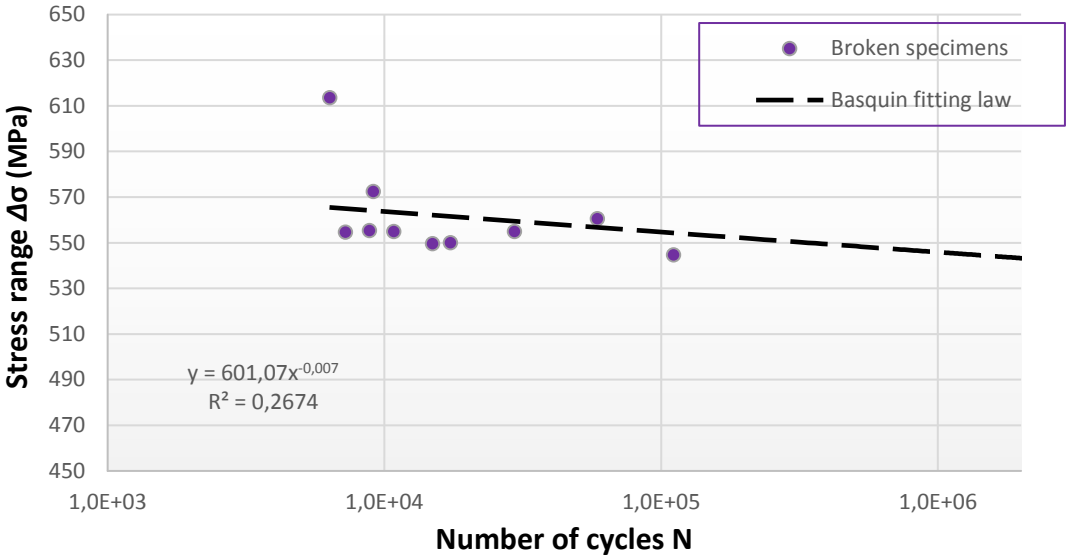

***Gráfico 3**. Curva S-N del acero S355J0 de la República Checa, información obtenida de [13]*

A partir de este gráfico, la tabla10 muestra los resultados experimentales a altos ciclos de carga.

República Checa [13]				
N [ciclos]	1.0E+04	1.0E+05	1.0E+06	1.0E+07
$\Delta\sigma$ [MPa]	563.540	554.530	545.663	536.939
$\Delta\sigma/\sigma_u$ σ_u=550 MPa	1.02	1	0.99	0.97

***Tabla 10**. Evaluación de la tensión a alto número de ciclos del acero S355J0 de la República Checa.*

El segundo espécimen utilizado ha sido un acero S355 de Portugal. La **Figura 4** muestra la geometría de la probeta utilizada en los ensayos y la **Tabla 11** especifica las dimensiones de la misma. La probeta posee una sección transversal S_0 de 30 mm^2.

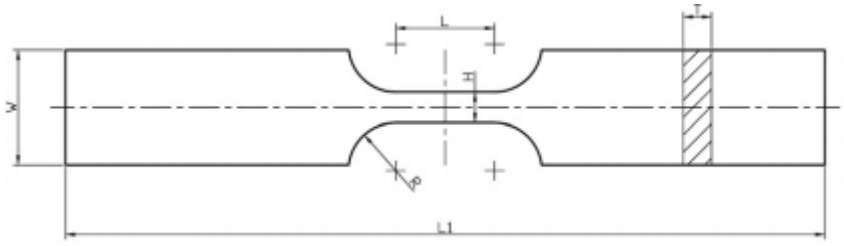

***Figura 4**. Geometría de la probeta plana hecha de acero S355 de Portugal, obtenida de [8]*

Specimen	W [mm]	T [mm]	L [mm]	L1 [mm]	H [mm]	R [mm]
S355	20	5	15	100	6	12

***Tabla 11**. Dimensiones de la probeta hecha de acero S355 de Portugal, información obtenida de [8]*

Los tests a fatiga fueron realizados utilizando cargas cíclicas con un ratio R=0. A su vez, los especímenes fueron ensayados con una fuerza de hasta 100 kN y una frecuencia que se ajustaba a los resultados.

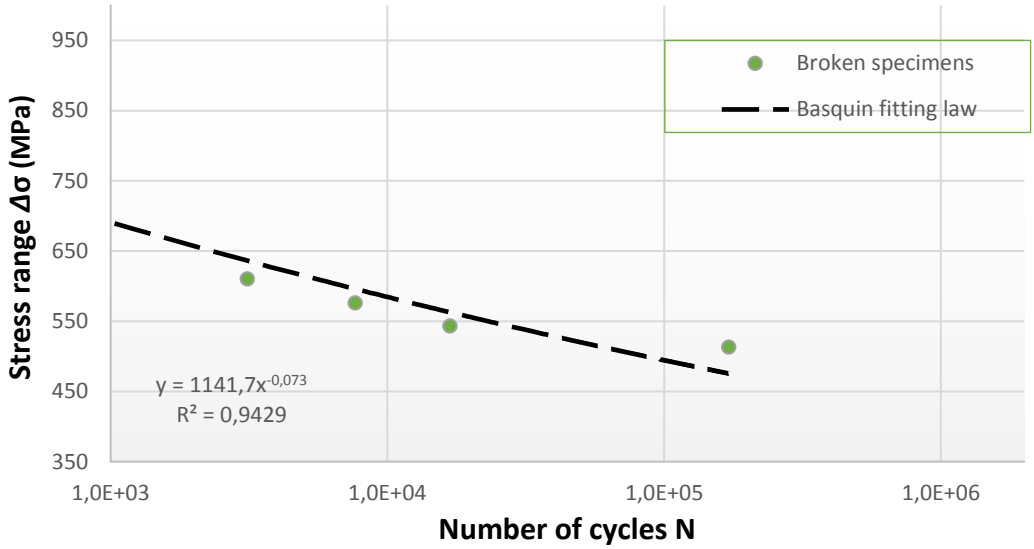

***Gráfico 4**. Curva S-N del acero S355 de Portugal, información obtenida de [8]*

Por ende, la **Tabla 12** muestra los resultados de los experimentos a altos ciclos:

Portugal [8]				
N [ciclos]	1.0E+04	1.0E+05	1.0E+06	1.0E+07
$\Delta\sigma$ [MPa]	582.843	492.665	-	-
$\Delta\sigma/\sigma_u$ σ_u=550 MPa	1.05	0.89	-	-

***Tabla 12**. Evaluación de la tensión a alto número de ciclos del acero S355 de Portugal.*

La tercera probeta utilizada en el estudio es un acero S355J2 proveniente de Alemania. La figura6 muestra la geometría de la probeta utilizada en los tests. A su vez, este espécimen posee una sección transversal S_0 de 960 mm^2.

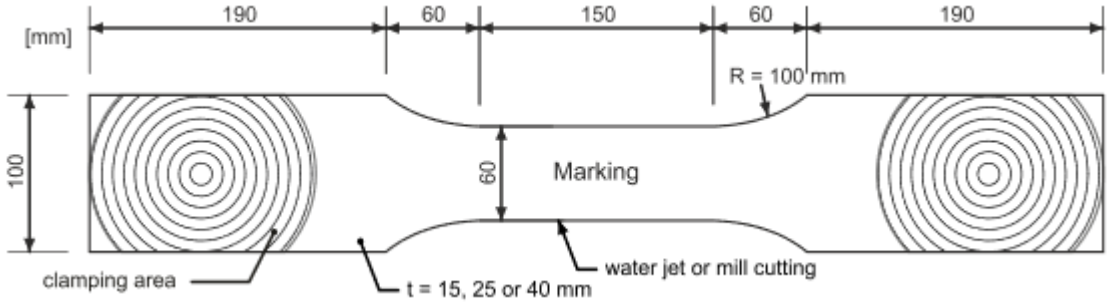

***Figura 5**. Geometría de la probeta plana hecha de acero S355J2 de Alemania, obtenida de [14]*

Los tests a fatiga han sido realizados utilizando cargas cíclicas con un ratio R=0.1. Las capacidades estáticas de la máquina se encontraban entre 1 MN y 1.6 MN. Dependiendo de la carga, la frecuencia podía variar entre 5 y 9 Hz.

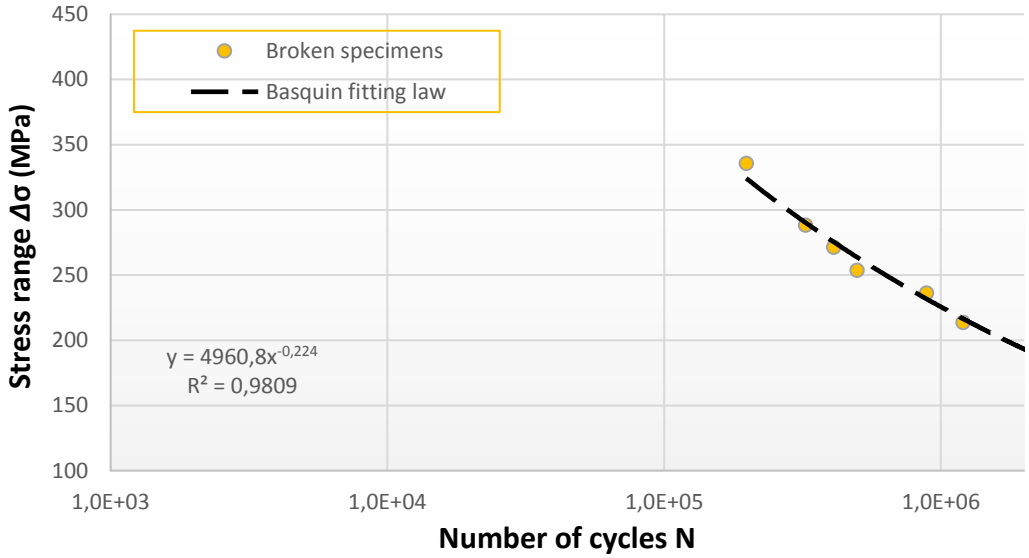

***Gráfico 5**. Curva S-N del acero S355J2 de Alemania, información obtenida de [14]*

De la misma manera, la **Tabla 13** muestra la evaluación de la tensión a altos ciclos:

Alemania [14]				
N [ciclos]	1.0E+04	1.0E+05	1.0E+06	1.0E+07
$\Delta\sigma$ [MPa]	-	376.315	224.673	134.137
$\Delta\sigma/\sigma_u$ σ_u=550 MPa	-	0.68	0.41	0.24

***Tabla 13**. Evaluación de la tensión a alto número de ciclos.del acero S355J2 de Alemania.*

Finalmente, la última probeta utilizada en el ensayo se trata de un acero S355 de Portugal. La **Figura 6** muestra la geometría de la probeta y la **Tabla 14** especifica las dimensiones de la misma. El espécimen posee una sección transversal S_0 de 93.75 mm^2.

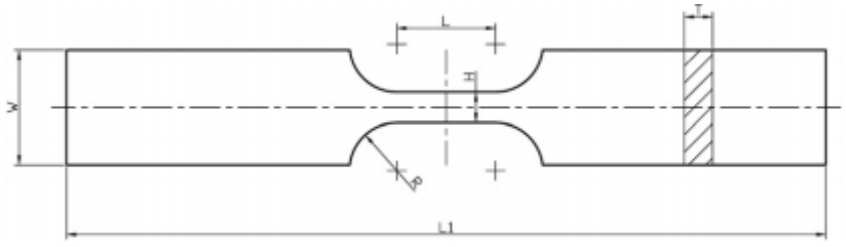

***Figura 6**. Geometría de la probeta plana hecha de acero S355 de portugal, obtenida de [12]*

Probeta	W [mm]	T [mm]	L [mm]	L1 [mm]	H [mm]	R [mm]
S355	30	7.5	26	200	12.5	8

***Tabla 14**. Dimensiones de la probeta de acero S355 de Portugal, información obtenida de [12]*

Los tests a fatiga fueron realizados utilizando cargas cíclicas con un ratio R=-1. Las probetas fueron ensayadas hasta una fuerza de 100 kN y una frecuencia que se ajustaba a los resultados.

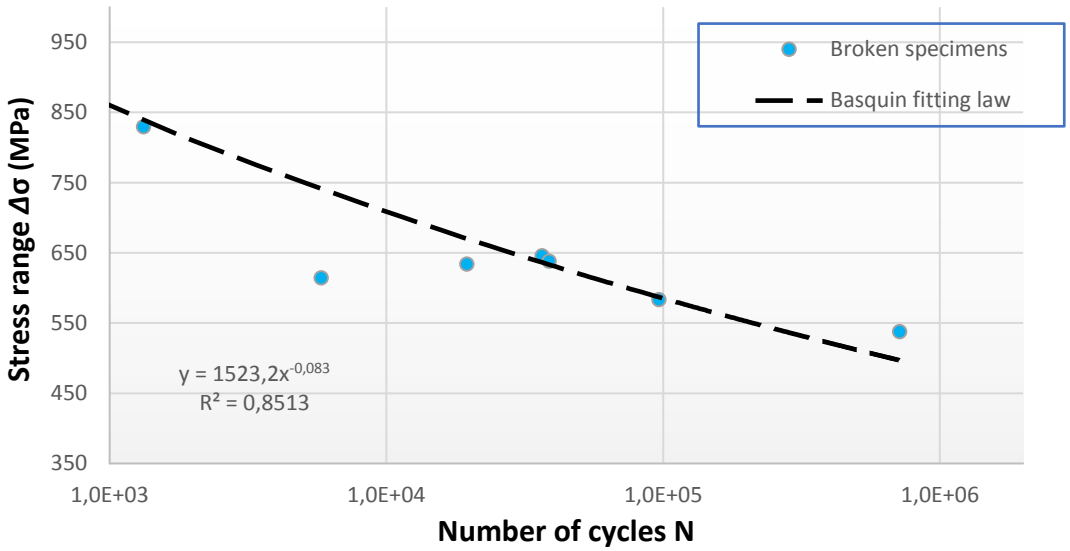

***Gráfico 6**. Curva S-N del acero S355 de Portugal, información obtenida de [12]*

En la **Tabla 15** se muestran los datos experimentales obtenidos a altos ciclos.

Portugal [12]				
N [ciclos]	1.0E+04	1.0E+05	1.0E+06	1.0E+07
Δσ [MPa]	709.180	585.810	-	-
$\Delta\sigma / \sigma_u$ σ_u=550 MPa	1.28	1.06	-	-

***Tabla 15**. Evaluación de la tensión a alto número de ciclos del acero S355 de Portugal.*

3.2.2 *Comparación de las curvas S-N de las probetas seleccionadas*

A pesar de haber obtenido varias probetas, la comparación de las curvas S-N de este acero no ha sido tan fácil. Esto se produce debido a que un factor esencial para la comparación de las propiedades a fatiga es el ratio (R). Es crucial que las probetas sean ensayadas con el mismo tipo de cargas cíclicas, ya que si no, la grieta por fatiga podría propagarse de una manera totalmente diferente.

Conociendo esto, las únicas probetas que cumplen los requisitos son el acero S355J0 de la República Checa y el acero S355J2 de Alemania, los cuales tienen el mismo ratio R=0.1.

La comparación de las curvas *S-N* de ambos aceros se encuentra presentada en el Gráfico 7:

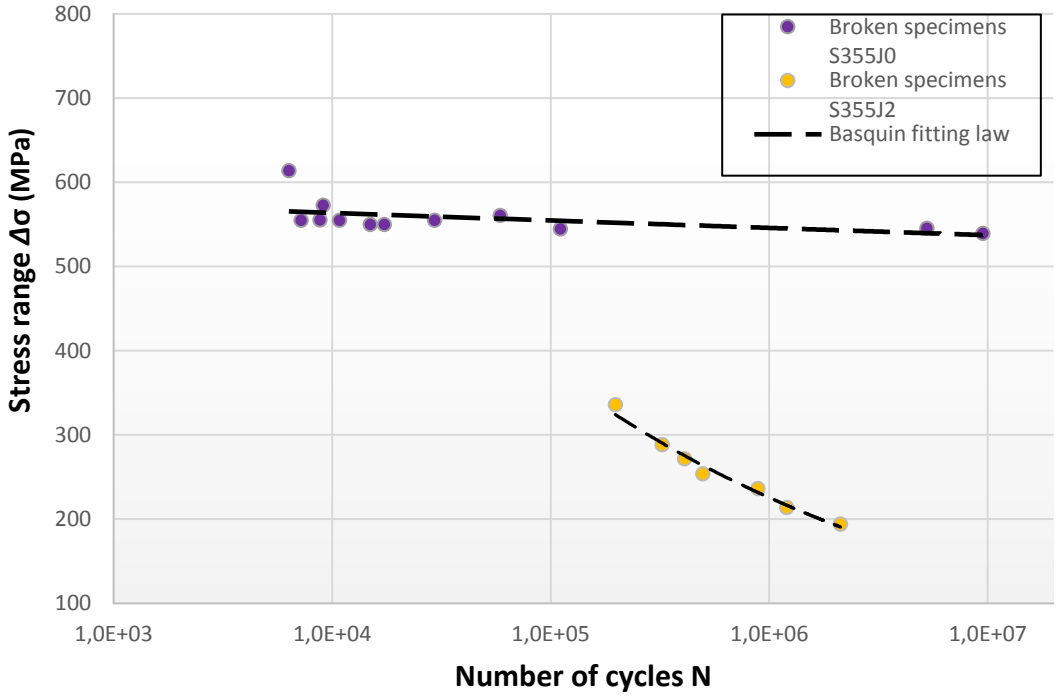

***Gráfico 7**. Comparativa de las curvas S-N de los aceros S355J0 de la República Checa [13] y S355J2 de Alemania [14] (R=0.1)*

Se puede observar claramente que existe una gran diferencia de tensiones entre ambas a alto número de ciclos.

3.2.3 Curva de propagación de la grieta

En este apartado, se muestra la comparación del crecimiento de la grieta a fatiga entre los especímenes S355J0 y S355J2 procedentes de la República Checa obtenidos a partir de resultados experimentales con las siguientes medidas:

L [mm]	W [mm]	B [mm]	a_n [mm]	H/2 [mm]	β_1
62.5	50	10	12.5	30	60°

***Tabla 16**. Medidas de los CT especímenes S355J0 y S355J2 [15]*

Los experimentos de crecimiento de la grieta han sido medidos a través de un ordenador preparado para mediciones con una fuerza de hasta 20 kN. Fueron utilizados un ratio *R*=0.1 para las cargas cíclicas y una frecuencia que variaba desde 96 (grietas más pequeñas) hasta 42 Hz (grietas más grandes).

En el Gráfico 8, la comparación de los resultados experimentales de los aceros S355J0 y S355J2 en la región de Paris es mostrada:

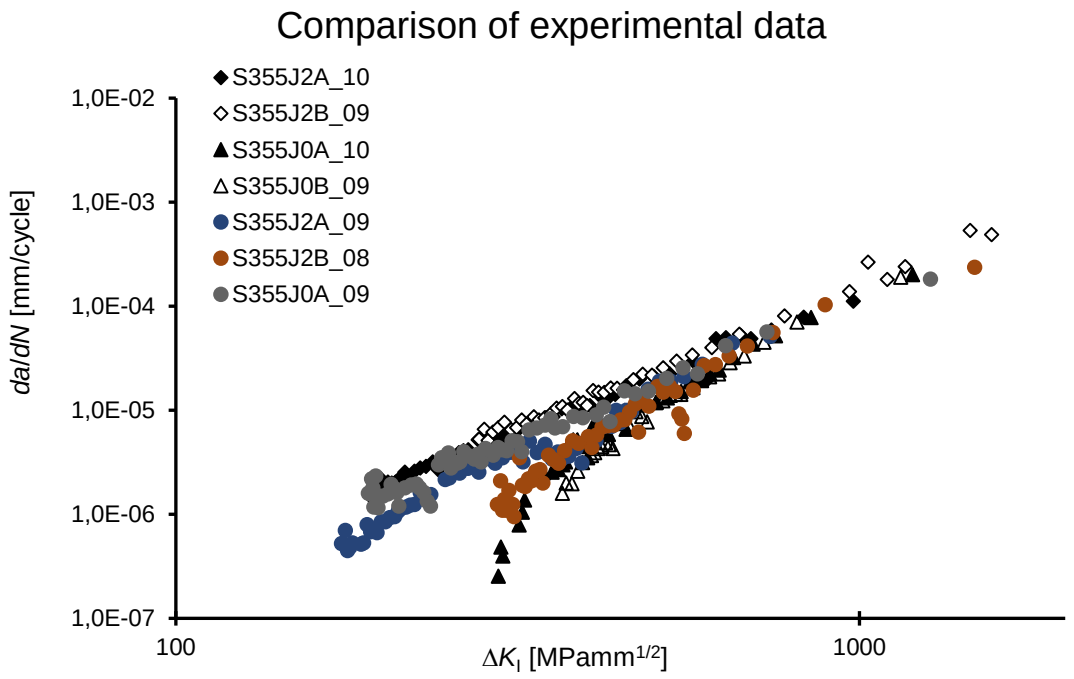

***Gráfico 8**. Resultados experimentales de las curvas de propagación de la grieta de los aceros S355J0 y S355J2, información obtenida de [15]*

En este gráfico podemos observar ambos crecimientos de la grieta, los cuales parecen ser similares.

La diferencia en el crecimiento de la grieta de los especímenes ensayados podría resultar de la diferente cantidad de partículas en la estructura del material y la influencia en la propagación de la grieta.

Las constantes *C* y *m* de los materiales fueron estimadas de los datos experimentales obtenidos en la región de Paris. Los resultados han sido colocados en la tabla18, junto con la información obtenida de Jesús et al. [12](Portugal) Y Adedipe (U.K.) [16].

Material	*C* [mm/cycle·MPa·$mm^{0.5}$]	*m* [-]
S355J2A	2.00E-12	2.595
S355J2B	1.00E-12	2.711
Adedipe S355J2 [16]	3.00E-14	3.296
S355J0A	2.00E-15	3.605
S355J0B	2.00E-15	3.638
De Jesús S355 [12]	3.00E-15	3.561

***Tabla 17.** Comparación de las constantes C y m a través de mediciones experimentales, información obtenida de S355J0 y S355J2 [15]*

Conclusiones

En este Trabajo de Fin de Grado, las propiedades estáticas y a fatiga de dos aceros estructurales S235 y S355 en varios países de la Unión Europea han sido analizadas y comparadas mediante información obtenida de experimentos y literatura.

Se han obtenido las siguientes conclusiones:

- La mayoría de la información recogida de la literatura de los aceros S235 y S355 estaba focalizada en las propiedades a fatiga de uniones soldadas.
- Existe poca información en artículos sobre el acero S235.
- Las mayores variaciones en las propiedades monotónicas de los aceros se encuentran en el S355J2G3.
- Diferencias en la composición química de los aceros podría ser producida por la composición del suelo de cada país.
- Las curvas *S-N* no pueden ser comparadas si el ratio *R* no tiene el mismo valor, ya que se producirían diferentes distribuciones de estrés en las probetas debido a que las cargas cíclicas no son iguales.
- La resistencia a fatiga de los materiales podría estar relacionada con las variaciones de la microestructura del material.
- Las propiedades a fatiga, en concreto la composición química, parece ser clave en el comportamiento a fatiga de los materiales.
- EL acero S355J2 muestra mayor curva de propagación de la grieta que el S355J0.
- El acero S355J2 muestra mayor límite de resistencia a fatiga.

Referencias

[1] WIRSCHING, Paul H. Statistical summaries of fatigue data for design purposes. 1983.

[2] Mesteel. (8/05/2019). Equivalents of Carbon Steel Qualities. Retaken from https://www.mesteel.com/qualities/equivalentscs.htm

[3] *EN 10025-2:2004* Hot rolled products of structural steels – Part2: Technical delivery conditions for non-alloy structural steels.

[4] ROBAKOWSKI, T.; CZUCHRYJ, J. The effect of overloading on the strength of St3W steel welded joints. *Welding International*, 1990, vol. 4, no 6, p. 425-429.

[5] BAYRAKTAR, E.; KAPLAN, D.; YILBAS, B. S. Comparative study: Mechanical and metallurgical aspects of tailored welded blanks (TWBs). *Journal of materials processing technology*, 2008, vol. 204, no 1-3, p. 440-450.

[6] HAN, Seungho, et al. Fatigue crack propagation near fatigue threshold in various structural steels. *Steel research*, 1996, vol. 67, no 12, p. 549-554.

[7] SŁOWIK, Jacek; ŁAGODA, Tadeusz. The fatigue life estimation of elements with circumferential notch under uniaxial state of loading. *International Journal of Fatigue*, 2011, vol. 33, no 9, p. 1304-1312.

[8] CARVALHO, D., et al. FATIGUE BEHAVIOUR OF STRUCTURAL STEELS. COMPARISON OF STRAIN-LIFE AND FATIGUE CRACK PROPAGATION DATA COMPORTAMENTO À FADIGA DE AÇOS ESTRUTURAIS. RELAÇÕES DEFORMAÇÃO-VIDA E TAXAS DE PROPAGAÇÃO DE FENDAS DE FADIGA.

[9] Estudio Experimental y Evaluación de Modelos de Plano Crítico en Fatiga Biaxial-Final Bachelor Thesis Ángel Rodríguez Ruiz.

[10] ROZUMEK, Dariusz; MACHA, Ewald. Opis rozwoju pęknięć zmęczeniowych w materiałach sprężysto-plastycznych przy proporcjonalnym zginaniu ze skręcaniem. Oficyna Wydawnicza Politechniki Opolskiej, 2006.

[11] CHIARELLI, M.; LANCIOTTI, Agostino; SACCHI, M. Effect of plasma cutting on the fatigue resistance of Fe510 D1 steel. *Journal of engineering materials and technology*, 2000, vol. 122, no 1, p. 141-145.

[12] DE JESUS, Abílio MP, et al. A comparison of the fatigue behavior between S355 and S690 steel grades. *Journal of Constructional Steel Research*, 2012, vol. 79, p. 140-150.

[13] SEITL, Stanislav, et al. Evaluation of fatigue properties of S355 J0 steel using ProFatigue and ProPagation software. *Procedia Structural Integrity*, 2018, vol. 13, p. 1494-1501.

[14] STRANGHÖNER, Natalie; JUNGBLUTH, Dominik. Fatigue strength of marked steel components. *Procedia Engineering*, 2015, vol. 133, p. 282-293.

[15] SEITL, Stanislav, et al. Comparison of the fatigue crack propagation rates in S355 J0 and S355 J2 steel grades. En *Key Engineering Materials*. Trans Tech Publications, 2018. p. 91-96.

[16] ADEDIPE, Oyewole; BRENNAN, Feargal; KOLIOS, Athanasios. Review of corrosion fatigue in offshore structures: Present status and challenges in the offshore wind sector. *Renewable and Sustainable Energy Reviews*, 2016, vol. 61, p. 141-154.

Lista de abreviaturas

ISO	International Organization of Standardization

Lista de símbolos

σ_y	Tensión de fluencia
σ_u	Tensión de rotura
E	Módulo de Young
A	Elongación
S_0	Sección transversal
υ	Coeficiente de Poisson
ε	Deformación
σ ó S	Tensión
N	Número de ciclos
σ_a	Tensión alterna
$\Delta\sigma$	Amplitud de tensión
R	Cociente de tensiones
N_f	Número de ciclos hasta rotura
CT	Compact tension
ΔK	Factor de intensidad de tensiones
ΔK_{th}	Umbral del factor de intensidad de tensiones
da/dN	Pendiente de la curva de velocidad de crecimiento
C, m	Constantes de la ley de Paris

Lista de figuras

Lista de gráficos

Lista de tablas